






RESEARCH ARTICLE | SEPTEMBER 23 2021

Complex viscosity of star-branched macromolecules from analytical general rigid bead-rod theory

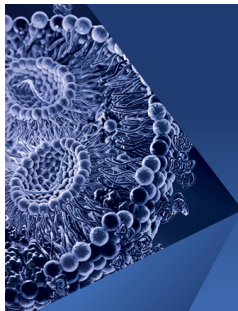
Special Collection: [Celebration of Robert Byron Bird \(1924-2020\)](#)

S. J. Coombs ; M. A. Kanso ; K. El Haddad ; A. J. Giacomin  

 Check for updates

Physics of Fluids 33, 093111 (2021)

<https://doi.org/10.1063/5.0063199>



Physics of Fluids

Special Topic:

Flow and Lipid Nanoparticles

Guest Editors: Richard Braatz and Mona Kanso

[Submit Today!](#)

Complex viscosity of star-branched macromolecules from analytical general rigid bead-rod theory

Cite as: Phys. Fluids **33**, 093111 (2021); doi: [10.1063/5.0063199](https://doi.org/10.1063/5.0063199)

Submitted: 13 July 2021 · Accepted: 24 July 2021 ·

Published Online: 23 September 2021



View Online



Export Citation



CrossMark

S. J. Coombs,¹  M. A. Kanso,¹  K. El Haddad,^{1,2}  and A. J. Giacomin^{1,3,4,5,a)} 

AFFILIATIONS

¹Chemical Engineering Department, Polymers Research Group, Queen's University, Kingston, Ontario K7L 3N6, Canada

²Baha and Walid Bassatne Department of Chemical Engineering and Advanced Energy, American University of Beirut, Beirut 1107 2020, Lebanon

³Mechanical and Materials Engineering Department, Queen's University, Kingston, Ontario K7L 3N6, Canada

⁴Physics, Engineering Physics and Astronomy Department, Queen's University, Kingston, Ontario K7L 3N6, Canada

⁵Mechanical Engineering Department, University of Nevada, Reno, Nevada 89557, USA

Note: This paper is part of the special topic, Celebration of Robert Byron Bird (1924-2020).

^{a)}Author to whom correspondence should be addressed: giacomin@queensu.ca

ABSTRACT

The complex viscosity of planar star-branched polymers has been derived from general rigid bead-rod theory, but only for singly-beaded arms. Here, we explore the respective roles of branch functionality, arm length, and nonplanar arrangements, analytically from general rigid bead-rod theory. For *nonplanar*, we include polyhedral, both regular and irregular. Further, for all structures, we compare with and without the central bead. We fit the theory to complex viscosity measurements on polybutadiene solutions, one quadrafunctional star-branched, the other unbranched, of the same molecular weight ($M_w = 200\,000$ g/gmol). We learn that when general rigid bead-rod theory is applied to quadrafunctional polybutadiene, a slightly irregular center-beaded *tetrahedron* of interior angle 134° is required (with $1\,360\,000$ g/gmol per bead) to describe its complex viscosity behavior.

Published under an exclusive license by AIP Publishing. <https://doi.org/10.1063/5.0063199>

I. INTRODUCTION

The complex viscosity of planar star-branched polymers has been derived from general rigid bead-rod theory, but only for singly-beaded arms (rows 3 and 4 of Table XV of Ref. 1 or Table 14 of Ref. 2). Though general rigid bead-rod theory has been applied to branched macromolecules structure-by-structure,^{1,3-5} ours is the first analytic to go beyond single-bead branching. Table I summarizes prior results on general formulas for planar macromolecules (see also Table 4 of Ref. 6) Table I improves upon previous tables by placing a common definition for N . In this paper, we explore the respective roles of branch functionality, arm length, and nonplanar arrangements of star-branched macromolecules analytically from general rigid bead-rod theory. By *analytically*, we mean that we begin with a geometric expression for the bead positions for a whole class of macromolecules. For this work, we chose general rigid bead-rod theory for its flexibility and accuracy (Sec. I of Ref. 1). General rigid bead-rod theory relies entirely on macromolecular orientation to explain complex viscosity

(Example 16.7-1 of Ref. 7). For nonplanar arrangements, we include polyhedral, both regular and irregular. For instance, measurements on 4-arm stars shall be compared specifically with *tetrahedral* rigid bead-rod models. Further, for all structures, planar or not, we compare with and without the central bead. We test our new theory against the seminal complex viscosity measurements of Refs. 8 and 9 on polybutadiene solutions, 4-arm star-branched vs unbranched. These references provide a unique comparison of the complex viscosities of polymer solutions, star-branched vs unbranched, of the same molecular weight.

We will compare our results with the control, the well-known result for the zero-shear viscosity of unbranched chains (row 1 of Table XV from Ref. 1 or Table 14 of Ref. 2),

$$\frac{\eta_0^\ell}{n^\ell kT\lambda_0} = \frac{1}{6}N(N^2 - 1). \quad (1)$$

Figure 1 defines the unbranched chain.

TABLE I. General formulas for planar macromolecules (TABLE XV of Ref. 1).

Macromolecule	$\frac{I_1}{mL^2}, \frac{I_2}{mL^2}$	$\frac{I_3}{mL^2}$	a	b	ν	$\frac{2b}{av}$	$\frac{\eta_0 - \eta_s}{nkT\lambda}$	$\frac{\lambda}{\lambda_0}$	$\frac{\Psi_{1,0}}{\lambda(\eta_0 - \eta_s)}$
Shish-kebab of N beads	$\frac{1}{12}N(N^2 - 1)$	0	$\frac{1}{90}N(N^2 - 1)$	$\frac{3}{5}$	$\frac{72}{N(N^2 - 1)}$	$\frac{3}{2}$	1	$\frac{1}{6}N(N^2 - 1)$	$\frac{6}{5}$
Rigid rings of N beads	$\frac{N}{8 \sin^2 \frac{\pi}{N}}$	$\frac{N}{4 \sin^2 \frac{\pi}{N}}$	$\frac{7N}{120 \sin^2 \frac{\pi}{N}}$	$\frac{3}{5}$	$\frac{48}{N} \sin^2 \frac{\pi}{N}$	$\frac{3}{7}$	2	$\frac{N}{4 \sin^2 \frac{\pi}{N}}$	$\frac{3}{5}$
Star-branched polymers with $N - 1$ branches and N beads ($4 \leq N \leq 7$)	$\frac{N - 1}{2}$	$N - 1$	$\frac{7}{30}(N - 1)$	$\frac{3}{5}$	$\frac{12}{N - 1}$	$\frac{3}{7}$	2	$N - 1$	$\frac{3}{5}$
Star-branched polymers with $N - 1$ branches and N beads ($N \geq 8$)	$\frac{N - 1}{8 \sin^2 \frac{\pi}{N - 1}}$	$\frac{N - 1}{4 \sin^2 \frac{\pi}{N - 1}}$	$\frac{7(N - 1)}{120 \sin^2 \frac{\pi}{N - 1}}$	$\frac{3}{5}$	$\frac{48}{N - 1} \sin^2 \frac{\pi}{N - 1}$	$\frac{3}{7}$	2	$\frac{N - 1}{4 \sin^2 \frac{\pi}{N - 1}}$	$\frac{3}{5}$

We will also compare our results with the well-known one for the relaxation time of unbranched chains (row 1 of Table XV of Ref. 1 or Table 14 of Ref. 2),

$$\frac{\lambda^\ell}{\lambda_0} \equiv \frac{1}{6}N(N^2 - 1), \tag{2}$$

wherein

$$N = N_A N_B + 1, \tag{3}$$

since we base our comparison on the seminal complex viscosity measurements of 8 and 9 on polybutadiene solutions, branched vs unbranched. We can introduce Eq. (3) because these measurements of 8 and 9 compare branched vs unbranched chains of the same molecular weight ($M_w = 200\,000$ g/gmol). Thus,

$$\frac{\lambda^\ell}{\lambda_0} \equiv \frac{1}{6}N_A N_B (N_A N_B + 1)(N_A N_B + 2), \tag{4}$$

where $M = m_i N$, where m_i is the bead mass, which branching does not change.

II. METHOD

We locate each bead of mass m_i with the position vector of the i th bead \mathbf{r}_i , where the macromolecular center of mass \mathbf{R} satisfies

$$\sum_{i=1}^N m_i (\mathbf{r}_i - \mathbf{R}) = 0, \tag{5}$$

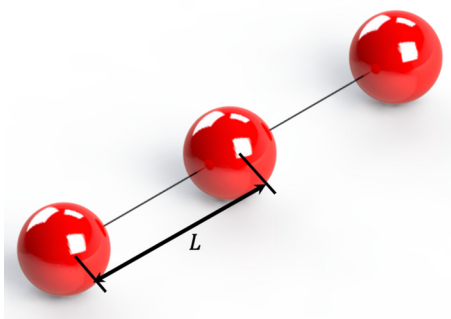


FIG 1. Defining L for a three-bead shish-kebab.

so that

$$\mathbf{R} = \frac{1}{M} \sum_{i=1}^N m_i \mathbf{r}_i, \tag{6}$$

where N is the total number of beads and $M \equiv \sum_{i=1}^N m_i$, the total mass. Since we construct our macromolecules, be they branched or not, with identical beads of diameter d and mass m , then $M \equiv mN$, and thus, the center of mass is

$$\mathbf{R} = \frac{1}{N} \sum_{i=1}^N \mathbf{r}_i, \tag{7}$$

which we will use below.

We next install *molecular coordinates*, at the macromolecular center of mass, and we orient these Cartesian coordinates such that δ_3 is along the polar axis of the *moment of inertia ellipsoid* (MIE).

The position vector of the i th bead with respect to the center of mass given by [Eqs. (16.7)–(16) of 7 or Eqs. (13.6)–(16) of Ref. 10],

$$\mathbf{R}_i \equiv [R_{i1}, R_{i2}, R_{i3}]. \tag{8}$$

For analytic general rigid bead-rod theory, Eq. (8) must be a geometric expression for the bead positions for a whole class of macromolecules. We can define the principal moments of inertia I_1 , I_2 , and I_3 by [Eqs. (16.7)–(17) and (16.7)–(18) of Ref. 7 or (13.6)–(17) and (13.6)–(18) of Ref. 10]

$$I_1 = m \sum_{i=1}^N (R_{i2}^2 + R_{i3}^2), \tag{9}$$

$$I_2 = m \sum_{i=1}^N (R_{i1}^2 + R_{i3}^2), \tag{10}$$

$$I_3 = 2m \sum_{i=1}^N R_{i1}^2, \tag{11}$$

where the subscript i is the bead number.

When the macromolecule is *oblate*

$$I_3 > I_1, \tag{12}$$

and for *prolate*

$$I_3 < I_1. \tag{13}$$

Our general rigid bead-rod theory just applies to axisymmetric macromolecules. By *axisymmetric*, we mean

$$I_1 = I_2. \tag{14}$$

For general rigid bead-rod theory, Hassager derives the expression for the shear relaxation function,

$$G(t - t') \equiv (2\eta_s + n\xi L^2 a)\delta(t - t') + nkTbe^{-(t-t')/\lambda}, \tag{15}$$

in which [Eqs. (16.7)–(38) of Ref. 11 or Eqs. (13.6)–(44), (13.6)–(45), and (13.6)–(46) of Ref. 12]

$$a \equiv \frac{2I_1 + I_3}{6mL^2} - \frac{(I_1 - I_3)^2}{5I_1 mL^2}, \tag{16}$$

$$b \equiv \frac{3(I_1 - I_3)^2}{5I_1^2}, \tag{17}$$

$$\nu \equiv \frac{6mL^2}{I_1}, \tag{18}$$

where [first paragraph of Sec. VI b, above Eq. (44) of Ref. 13]

$$0 \leq b \leq \frac{3}{5}. \tag{19}$$

The three quantities a , b , and ν thus define completely the differences in linear viscoelastic behaviors arising between different axisymmetric macromolecular structures. Whereas we associate a with the Dirac delta function contribution to the relaxation function, we associate b with the dying exponential.

From Fig. 3 of Ref. 1, for all axisymmetric macromolecules, we glean the companion to Eq. (19),

$$\frac{4}{5} < a\nu < \frac{77}{24}, \tag{20}$$

and since $\nu > 0$ [see its definition, Eq. (18)], $a > 0$. Combining this with Eq. (16) yields, for all axisymmetric macromolecules,

$$\frac{(I_1 - I_3)^2}{I_1(2I_1 + I_3)} < \frac{5}{6}, \tag{21}$$

which is new.

The macromolecular relaxation time can be expressed as

$$\lambda \equiv \frac{\xi I_1}{6mkT} \equiv \frac{\xi L^2}{\nu kT}, \tag{22}$$

where the bead friction coefficient is

$$\xi \equiv 3\pi d\eta_s, \tag{23}$$

and, for the rigid dumbbell [Eq. (6) of Ref. 14],

$$\lambda_0 \equiv \frac{\xi L^2}{12kT} \equiv \frac{\pi d\eta_s L^2}{4kT}, \tag{24}$$

and where Figs. 1–5 define center-to-center distances between nearest neighbors, L .

Macromolecular lopsidedness, $2b/a\nu$, is the extent to which the branched macromolecule deviates from a spherically symmetrical structure,

$$0 \leq \frac{2b}{a\nu} \leq \frac{3}{2}. \tag{25}$$

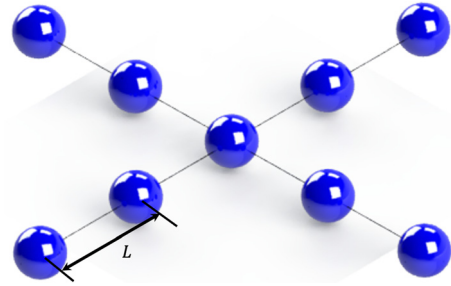


FIG. 2. Defining L when $3 \leq N_A \leq 6$ in a center-beaded planar star-branched macromolecule. Specific example $N_A = 4$, $N_B = 2$.

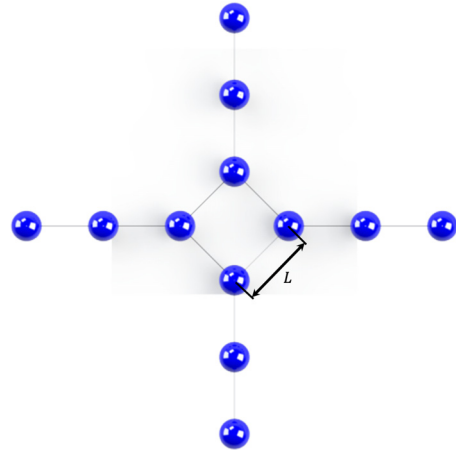


FIG. 3. Defining L when $3 \leq N_A \leq 6$ in a center-ringed planar star-branched macromolecule. Specific example $N_A = 4$, $N_B = 3$.

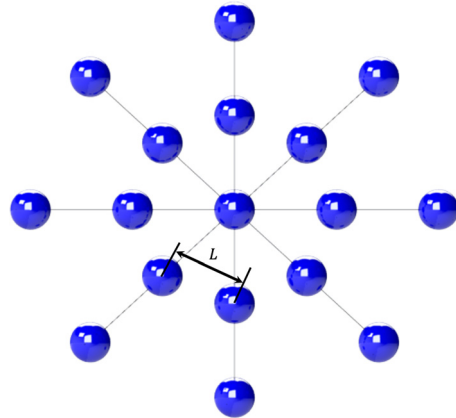


FIG. 4. Defining L when $N_A \leq 7$ center-beaded planar star-branched macromolecule. Specific example $N_A = 8$, $N_B = 2$.

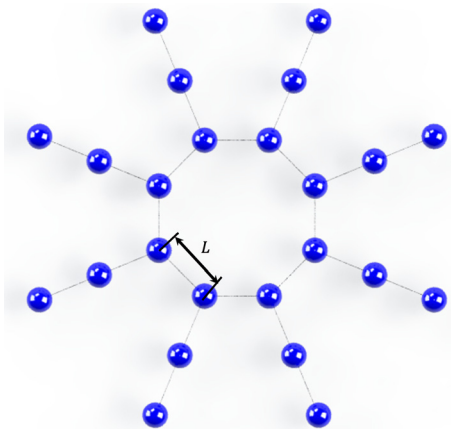


FIG. 5. Defining L when $N_A \leq 7$ center-ringed planar star-branched macromolecule. Specific example $N_A = 8, N_B = 3$.

The minimum value of 0 is for spherically symmetrical branched structures such as the symmetric rigid octahedron, and the maximum value is $3/2$ for long slender bodies such as the rigid dumbbell or the multibead-rod, also known as “shish-kebab.”¹ Dividing Eqs. (22) by Eq. (24) normalizes the relaxation time of the general macromolecule to that of the simplest,

$$\frac{\lambda}{\lambda_0} \equiv \frac{12}{\nu}. \tag{26}$$

We can then use Eq. (15) to calculate the polymer contribution to the stress tensor in any linear viscoelastic flow, including oscillatory shear flow, from Eq. (1) of Ref. 15,

$$\tau_p \equiv - \int_{-\infty}^t G(t-t') \dot{\gamma}(t') dt', \tag{27}$$

where all symbols are defined in Tables II and III.

A. Oscillatory shear flow

We measure the complex viscosity in oscillatory shear flow, generated by confining the fluid to a simple shear apparatus and then by subjecting one solid–liquid boundary to a coplanar sinusoidal displacement generating the corresponding cosinusoidal shear rate,

$$\dot{\gamma}(t) = \dot{\gamma}^0 \cos \omega t, \tag{28}$$

such that, the rate of deformation tensor is given by

$$\dot{\gamma}(\mathbf{t}) = \begin{bmatrix} 0 & \dot{\gamma}^0 \cos \omega t & 0 \\ \dot{\gamma}^0 \cos \omega t & 0 & 0 \\ 0 & 0 & 0 \end{bmatrix}. \tag{29}$$

Using the characteristic relaxation time of the branched polymeric viscoelastic fluid, λ , we can nondimensionalize Eq. (28) as

$$\lambda \dot{\gamma}(t) = \lambda \dot{\gamma}^0 \cos \lambda \omega (t/\lambda), \tag{30}$$

where $\lambda \omega$ and $\lambda \dot{\gamma}^0$ are the Deborah and Weissenberg numbers. In this paper, we focus on small-amplitude oscillatory shear flow (SAOS).

TABLE II. Dimensional variables. Legend: $M \equiv$ mass, $L \equiv$ length, $t \equiv$ time.

Name	Symbol	Dimensions
Angular frequency	ω	t^{-1}
Bead center-to-center distances between nearest neighbors	L	L
Bead diameter	d	L
Bead friction coefficient	ξ	M/t
Cartesian coordinates	x, y, z	L
Complex viscosity	η^*	M/Lt
Complex viscosity, <i>minus</i> imaginary part	η''	M/Lt
Complex viscosity, <i>minus</i> imaginary part at high frequency	η''_∞	M/Lt
Complex viscosity, real part	η'	M/Lt
Complex viscosity, real part at high frequency	η'_∞	M/Lt
Complex viscosity, solvent	η_s	M/Lt
Complex viscosity, zero-shear of linear macromolecules	η_0^l	M/Lt
Complex viscosity, zero-shear of <i>minus</i> imaginary part	η_0''	M/Lt
Complex viscosity, zero-shear of real part	η_0'	M/Lt
Element for Kronecker delta	$\delta(s)$	t^{-1}
Energy values in molecular-scale systems	kT	ML^2/t^2
First, second normal stress coefficient, small-amplitude oscillatory shear response, displacement term	Ψ_1^d, Ψ_2^d	M/L
First, second normal stress coefficient, in-phase with $\cos 2\omega t$, for small-amplitude oscillatory shear response	Ψ_1', Ψ_2'	M/L
First, second normal stress coefficient, out-of-phase with $\cos 2\omega t$, for small-amplitude oscillatory shear response	Ψ_1'', Ψ_2''	M/L
First, second normal stress coefficient, complex	Ψ_1^*, Ψ_2^*	M/L
Macromolecular center of mass	\mathbf{R}	L
Mass of each bead	m_i	M
Molecular weight	M_w	M/mole
Moments of inertia	I_1, I_2, I_3	ML^2
Number of dumbbells per unit volume	n	$1/L^3$
Number of dumbbells per unit volume, unbranched chain	n^ℓ	$1/L^3$
Polymer contribution to the extra stress tensor	τ_p	M/Lt^2
Position vector of the i th bead with respect to the center of mass	\mathbf{R}_i	L
Position vector with respect to the center of mass for each bead of a planar star on the n th arm	$\mathbf{R}_{n,c}$	L
Position vector of the i th bead	\mathbf{r}_i	L
Rate of deformation tensor	$\dot{\gamma}(t)$	t^{-1}
Relaxation time of a rigid dumbbell	λ_0	t

TABLE II. (Continued.)

Name	Symbol	Dimensions
Relaxation time of solution	λ	t
Relaxation time of unbranched solution	λ^ℓ	t
Spherical coordinates, radial distance	r	L
Shear rate amplitude	$\dot{\gamma}^0$	t^{-1}
Shear rate at specific time	$\dot{\gamma}(t')$	t^{-1}
Shear rate	$\dot{\gamma}(t)$	t^{-1}
Shear relaxation function	$G(t - t')$	M/Lt^2
Time, past	t'	t
Time, current	t	t
Time, interval of past	$(t - t')$	t
Total mass	M	M
Velocity vector	\mathbf{v}	L/t

For this flow field, for the molecular definition of *small amplitude*, general rigid bead-rod theory yields

$$\lambda \dot{\gamma}^0 \ll \frac{1}{\nu \sqrt{2}}, \quad (31)$$

whose left side is the macromolecular Weissenberg number. From Eq. (31), we learn that branched structures with higher ν will have lower limits for linear viscoelasticity.

TABLE III. Dimensionless variables and groups.

Name	Symbol	Range
Architectural constants	a, b, ν	>0
Arm number	n	≥ 0
Bead number along each branch	c	≥ 0
Bead position for irregular tetrahedral, spherical coordinates	θ_1	$\sin^{-1} \frac{d}{2L} \leq \theta_1 \leq \frac{\pi}{2}$
Bead volume fraction	ϕ	≥ 0
Branch angle	θ_n	$1 \leq n \leq N_A$
Cartesian coordinates with respect to the center of mass	$\hat{\delta}_1, \hat{\delta}_2, \hat{\delta}_3$	
Concentration factor	$\frac{n^\ell \eta_0}{m \eta_0^\ell}$	>0
Coefficient in Eqs. (56)–(58)	Z, α, β	≥ 0
Coefficients in Eqs. (105)–(107)	α_c, β_c	≥ 0
Deborah number	$\lambda\omega$	≥ 0
Lopsidedness	$2b/av$	>0
Number of arms on the macromolecules	N_A	≥ 0
Number of beads on each arm on the macromolecule	N_B	≥ 0
Spherical coordinates, azimuthal angle	ϕ	$0 \leq \phi \leq 2\pi$
Spherical coordinates, polar angle	θ	$0 \leq \theta \leq \pi$
Tetrahedral angle	Θ_t	1.91 rad
Total number of beads	N	>0

In oscillatory shear flow, polymeric liquids respond with shear stress, and also with normal stress differences. When Eq. (31) is satisfied, the shear stress response is sinusoidal,

$$\tau_{21} = -\dot{\gamma}^0 (\eta'(\omega) \cos \omega t + \eta''(\omega) \sin \omega t), \quad (32)$$

with parts in-phase and out-of-phase with the shear rate.⁵ We follow the Gemant convention^{16–18}

$$\eta^* \equiv \eta' - i\eta''. \quad (33)$$

Substituting Eq. (26) of Refs. 1 and 2, for general rigid bead-rod theory, for the polymer contribution to the real part of the complex viscosity, we get

$$\frac{(\eta' - \eta_s)}{nkT\lambda_0} = 6a \left\{ 1 + \frac{2b}{av} \left(\frac{1}{1 + (\lambda\omega)^2} \right) \right\}, \quad (34)$$

and for *minus* the imaginary part [Eq. (34) of Ref. 1],

$$\frac{\eta''}{nkT\lambda_0} = 6a \left\{ \frac{2b}{av} \frac{\lambda\omega}{1 + (\lambda\omega)^2} \right\}, \quad (35)$$

from which we learn that $b > 0$ is necessary for the fluid to exhibit elasticity in oscillatory shear flow. In other words, the decaying exponential term in Eq. (15) is the source of the fluid elasticity. From Eqs. (34) and (35), both η' and η'' are amplified by the same factor $1/nkT\lambda_0$.

Equations (34) and (35) are subject to inequalities Eq. (19) for b , and (below Tables 16.7–1 of Ref. 7) and Eq. (25) for the macromolecular lopsidedness. As $\lambda\omega \rightarrow 0$, Eqs. (34) and (35) give

$$\frac{(\eta_0 - \eta_s)}{nkT\lambda_0} \equiv \lim_{\lambda\omega \rightarrow 0} \frac{(\eta' - \eta_s)}{nkT\lambda_0} = 6a \left\{ 1 + \frac{2b}{av} \right\}, \quad (36)$$

$$\frac{\eta''_0}{nkT\lambda_0} \equiv \lim_{\lambda\omega \rightarrow 0} \frac{\eta''}{nkT\lambda_0} = 0, \quad (37)$$

and, as $\lambda\omega \rightarrow \infty$,

$$\frac{(\eta'_\infty - \eta_s)}{nkT\lambda_0} \equiv \lim_{\lambda\omega \rightarrow \infty} \frac{(\eta' - \eta_s)}{nkT\lambda_0} = 6a, \quad (38)$$

$$\frac{\eta''_\infty}{nkT\lambda_0} \equiv \lim_{\lambda\omega \rightarrow \infty} \frac{\eta''}{nkT\lambda_0} = 0, \quad (39)$$

where limits, Eqs. (36) and (38), are subject to Eqs. (19) and (25).

Nondimensionalizing Eqs. (34) and (35) with Eq. (36) yields

$$\frac{\eta' - \eta_s}{\eta_0 - \eta_s} = \left\{ 1 + \frac{2b}{av} \right\}^{-1} \left\{ 1 + \frac{2b}{av} \left(\frac{1}{1 + (\lambda\omega)^2} \right) \right\} \quad (40)$$

and

$$\frac{\eta''}{\eta_0 - \eta_s} = \left\{ 1 + \frac{2b}{av} \right\}^{-1} \left\{ \frac{2b}{av} \frac{\lambda\omega}{1 + (\lambda\omega)^2} \right\}, \quad (41)$$

which are universal results from general rigid bead-rod theory, applying to any suspension of axisymmetric macromolecules. In this work, we will derive special cases of Eqs. (40) and (41) for suspensions of star-branched polymers, be they center-beaded or center-ringed.

Solving Eq. (34) for the real part of the complex viscosity, we get

$$\frac{\eta'}{nkT\lambda_0} = 6a \left\{ 1 + \frac{2b}{a\nu} \left(\frac{1}{1 + (\lambda\omega)^2} \right) \right\} + \frac{\eta_s}{nkT\lambda_0}, \quad (42)$$

and if

$$\frac{\eta_s}{nkT\lambda_0} \ll 6a, \quad (43)$$

then solvent viscosity does not matter. Since the left side of Eq. (43) does not contain macromolecular constants, that is, neither a , nor b , nor ν , we see that the negligibility of solvent viscosity does not depend on the branching structure. When Eq. (43) obtains, we get

$$\frac{\eta'}{nkT\lambda_0} = 6a \left\{ 1 + \frac{2b}{a\nu} \left(\frac{1}{1 + (\lambda\omega)^2} \right) \right\}, \quad (44)$$

which we will use presently.

Inserting row 1 of Table I (or of Table XV of Ref. 1) into Eqs. (44) and (35) yields, for unbranched chains ($N = N_A N_B + 1$),

$$\frac{\eta'}{nkT\lambda_0} = \frac{1}{15} N_A N_B (N_A N_B + 1) (N_A N_B + 2) \left\{ 1 + \frac{3}{2} \left(\frac{1}{1 + (\lambda\omega)^2} \right) \right\} \quad (45)$$

and

$$\frac{\eta''}{nkT\lambda_0} = \frac{1}{15} N_A N_B (N_A N_B + 1) (N_A N_B + 2) \left\{ \frac{3}{2} \frac{\lambda\omega}{1 + (\lambda\omega)^2} \right\}. \quad (46)$$

As Eq. (45) $\lambda\omega \rightarrow 0$,

$$\frac{\eta'_0}{nkT\lambda_0} = \frac{1}{6} N_A N_B (N_A N_B + 1) (N_A N_B + 2), \quad (47)$$

so that

$$\frac{\eta'}{\eta'_0} = \frac{2}{5} + \frac{3}{5} \left\{ \frac{1}{1 + (\lambda\omega)^2} \right\} \quad (48)$$

and

$$\frac{\eta''}{\eta''_0} = \frac{3}{5} \left\{ \frac{\lambda\omega}{1 + (\lambda\omega)^2} \right\}, \quad (49)$$

which we will use to normalize our new results for star-branched polymers below.

III. RESULTS: PLANAR STARS

For equidimensional branching, the total number of beads in a center-beaded planar star is given by Eq. (3), and in a center-ringed one,

$$N = N_A N_B, \quad (50)$$

where N_A is the total number of arms on the macromolecule, N_B , the number of beads on an arm (excluding the center bead), and the product $N_A N_B$ is thus always a multiple of N_A .

For $3 \leq N_A \leq 6$, we position our Cartesian molecular z -axis normal to and centered on the planar star. The position vector with

respect to the center of mass for each bead of a planar star on the n th arm is given by [Eqs. (16.7)–(17) of Ref. 10 or Eqs. (13.6)–(17) of Ref. 19]

$$\mathbf{R}_{n,c} = [cL \cos \theta_n, cL \sin \theta_n, 0], \quad (51)$$

where the first arm, $n = 1$, is along our molecular x -axis, with arms following counterclockwise enumeration, and c is the bead number along each branch, counted radially from the center ($c = 0$). Figures 2 and 3 illustrate these definitions. The branch angle, measured counterclockwise in the plane of the star, and from our molecular x -axis, is given by

$$\theta_n = (n - 1) \frac{2\pi}{N_A}, \quad (52)$$

which is subject to

$$1 \leq n \leq N_A, \quad (53)$$

which we will use presently. In Subsections III A–III D, we examine center-beaded planar stars and their center-ringed counterparts. Since all planar stars are oblate, Eq. (12) applies to Subsections III A–III D. Otherwise put, $N_B > 2$.

For $N_A \geq 7$, we position our Cartesian molecular z -axis normal to and centered on the planar star. The position vector with respect to the center of mass for each bead of a planar star on the n th arm is given by [Eqs. (16.7)–(17) of Ref. 10 or Eqs. (13.6)–(17) of Ref. 19]

$$\mathbf{R}_{n,c} = \left[cL \frac{\cos \theta_n}{2 \sin \left(\frac{\pi}{N_A} \right)}, cL \frac{\sin \theta_n}{2 \sin \left(\frac{\pi}{N_A} \right)}, 0 \right], \quad (54)$$

where the first arm, $n = 1$, is along our molecular x -axis, with arms following counterclockwise enumeration, and c is the bead number along each branch, counted radially from the center ($c = 0$). Figures 4 and 5 illustrate these definitions.

A. Center-beaded planar stars ($3 \leq N_A \leq 6$)

For center-beaded planar stars, Eqs. (51) and (52) are subject to Eqs. (53) and

$$1 \leq c \leq N_B. \quad (55)$$

Substituting Eq. (51) into Eqs. (9)–(11), we get the principal moments of inertia for a center-beaded planar star,

$$I_1 \equiv mL^2 \sum_{c=1}^{c=N_B} c^2 \sum_{n=1}^{n=N_A} \sin^2 \theta_n \equiv mL^2 Z\alpha, \quad (56)$$

$$I_2 \equiv mL^2 \sum_{c=1}^{c=N_B} c^2 \sum_{n=1}^{n=N_A} \cos^2 \theta_n \equiv mL^2 Z\beta, \quad (57)$$

$$I_3 \equiv 2mL^2 \sum_{c=1}^{c=N_B} c^2 \sum_{n=1}^{n=N_A} \cos^2 \theta_n \equiv 2mL^2 Z\beta. \quad (58)$$

From Eqs. (52) and (56)–(58), we get

$$Z \equiv \sum_{c=1}^{c=N_B} c^2 = N_B (N_B + 1) (2N_B + 1), \quad (59)$$

$$\alpha \equiv \sum_{n=1}^{n=N_A} \sin^2 \theta_n = \sum_{n=1}^{n=N_A} \sin^2 \left[(n-1) \frac{2\pi}{N_A} \right] = \frac{N_A}{2}, \quad (60)$$

$$\beta \equiv \sum_{n=1}^{n=N_A} \cos^2 \theta_n = \sum_{n=1}^{n=N_A} \cos^2 \left[(n-1) \frac{2\pi}{N_A} \right] = \frac{N_A}{2} = \alpha. \quad (61)$$

Substituting Eqs. (59) and (60) into Eq. (56) gives

$$I_1 \equiv \frac{N_A}{2} N_B (N_B + 1) (2N_B + 1) mL^2, \quad (62)$$

and Eqs. (59) and (61) into Eq. (57),

$$I_2 \equiv \frac{N_A}{2} N_B (N_B + 1) (2N_B + 1) mL^2 = I_1, \quad (63)$$

and Eqs. (59) and (61) into Eq. (58),

$$I_3 \equiv N_A N_B (N_B + 1) (2N_B + 1) mL^2. \quad (64)$$

Substituting Eqs. (62)–(64) into Eqs. (16)–(18) gives the orientation constants for a center-beaded planar star-branched polymer,

$$a \equiv \frac{7}{30} N_A N_B (N_B + 1) (2N_B + 1), \quad (65)$$

$$b \equiv \frac{3}{5}, \quad (66)$$

$$\nu \equiv \frac{12}{N_A N_B (N_B + 1) (2N_B + 1)}. \quad (67)$$

Multiplying a by ν gives

$$a\nu = \frac{14}{5}, \quad (68)$$

as it must, for $b = 3/5$ (see Fig. 3 of Ref. 1). Inserting Eq. (67) into Eq. (26) yields

$$\frac{\lambda}{\lambda_0} \equiv N_A N_B (N_B + 1) (2N_B + 1), \quad (69)$$

for center-beaded stars with $3 \leq N_A \leq 6$.

Equations (65)–(67) are subject to Eq. (21). Substituting Eqs. (66) and (68) into Eqs. (40) and (41) yields, for suspensions of center-beaded planar star-branched polymers,

$$\frac{\eta' - \eta_s}{\eta_0 - \eta_s} = \frac{7}{10} \left\{ 1 + \frac{3}{7} \left(\frac{1}{1 + (\lambda\omega)^2} \right) \right\}, \quad (70)$$

and

$$\frac{\eta''}{\eta_0 - \eta_s} = \frac{3}{10} \left\{ \frac{\lambda\omega}{1 + (\lambda\omega)^2} \right\}, \quad (71)$$

which we will recover, from time to time, below. Equations (70) and (71) are special cases of Eqs. (40) and (41).

Substituting Eqs. (62) and (64) into Eq. (21) gives, for all center-beaded planar stars,

$$\frac{1}{4} < \frac{5}{6}, \quad (72)$$

as it should.

The uninitiated might expect the special case of the N -bead shish-kebab, namely, the 2-arm center-beaded star with $\frac{1}{2}(N - 1)$

beads on each arm [$N_A = 2, N_B = \frac{1}{2}(N - 1)$] to be relevant here. However, whereas all planar stars are oblate, all shish-kebabs are prolate.

For Eqs. (65) and (67), we next examine their special cases of the N -bead star-branched polymer, with single-beaded arms ($N_A = N - 1, N_B = 1$),

$$a \equiv \frac{7}{30} (N - 1), \quad (73)$$

and

$$\nu \equiv \frac{12}{N - 1}, \quad (74)$$

which match row 3 of Table I (or row 3 of Table XV of Ref. 1) as they must.

Substituting Eqs. (65)–(67) into Eqs. (44) and (35),

$$\frac{\eta'}{nkT\lambda_0} = \left[\frac{7}{5} (N_A N_B (N_B + 1) (2N_B + 1)) \right] \left\{ 1 + \frac{3}{7} \left(\frac{1}{1 + (\lambda\omega)^2} \right) \right\}, \quad (75)$$

$$\frac{\eta''}{nkT\lambda_0} = \left[\frac{7}{5} (N_A N_B (N_B + 1) (2N_B + 1)) \right] \left\{ \frac{3}{7} \frac{\lambda\omega}{1 + (\lambda\omega)^2} \right\}, \quad (76)$$

as $\lambda\omega \rightarrow 0$

$$\frac{\eta_0}{nkT\lambda_0} = 2N_A N_B (N_B + 1) (2N_B + 1), \quad (77)$$

so that

$$\frac{\eta'}{\eta_0} = \frac{7}{10} \left\{ 1 + \frac{3}{7} \left(\frac{1}{1 + (\lambda\omega)^2} \right) \right\} \quad (78)$$

and

$$\frac{\eta''}{\eta_0} = \frac{3}{10} \left\{ \frac{\lambda\omega}{1 + (\lambda\omega)^2} \right\}, \quad (79)$$

illustrated in Figs. 6 and 7, which expand as

$$\frac{\eta'}{\eta_0} = 1 - \frac{3}{10} [(\lambda\omega)^2 - (\lambda\omega)^4 + \dots] \quad (80)$$

and

$$\frac{\eta''}{\eta_0} = \frac{3}{10} [\lambda\omega - (\lambda\omega)^3 + \dots]. \quad (81)$$

From the $(\lambda\omega)^2$ and $\lambda\omega$ terms of Eqs. (80) and (81), respectively, we learn about how (and how quickly) our center-beaded star suspension departs from its Newtonian equilibrium behavior. Equations (78) and (79) are special cases of Eqs. (70) and (71), where $\eta_0 \gg \eta_s$. From Eqs. (78) and (79), we learn that for all planar center-beaded star suspensions, from general rigid bead-rod theory, both the real and imaginary parts of the complex viscosity share the same shapes for their frequency dependencies. Otherwise put, differences between star architectures shall just manifest in their λ and η_0 [following Eqs. (69) and (77) for $3 \leq N_A \leq 6$].

To deepen our understanding of how branching affects the rheology of center-beaded planar stars ($3 \leq N_A \leq 6$), we can normalize our main result, Eq. (77), with Eq. (47),

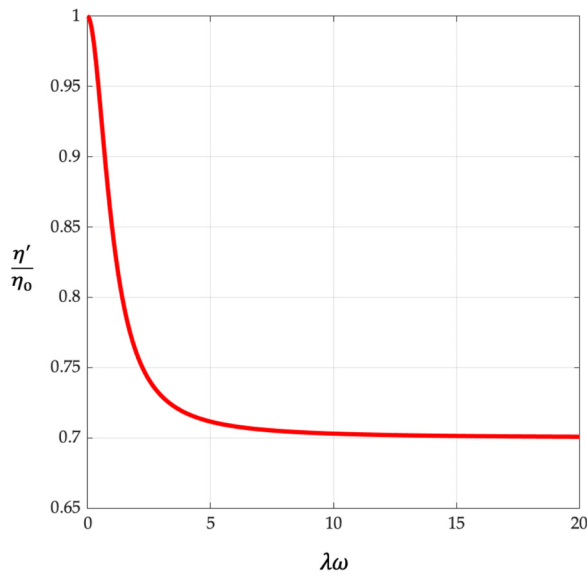


FIG. 6. $\eta'/\eta_0(\lambda\omega)$ from Eq. (78) for center-beaded and center-ringed planar stars.

$$\frac{n^\ell \eta_0}{n \eta_0^\ell} = \frac{12(N_B + 1)(2N_B + 1)}{(N_A N_B + 1)(N_A N_B + 2)}, \tag{82}$$

and Eq. (69), with Eq. (4),

$$\frac{\lambda}{\lambda^\ell} = \frac{6(N_B + 1)(2N_B + 1)}{(N_A N_B + 1)(N_A N_B + 2)}, \tag{83}$$

where the superscripted ℓ indicates unbranched.

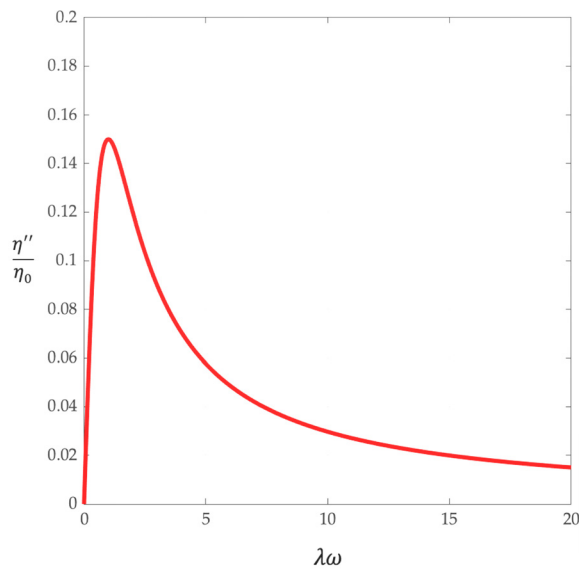


FIG. 7. $\eta''/\eta_0(\lambda\omega)$ from Eq. (79) for center-beaded and center-ringed planar stars.

B. Center-ringed planar stars ($3 \leq N_A \leq 6$)

For center-ringed planar stars, Eqs. (51) and (52) are subject to Eqs. (53) and

$$2 \leq c \leq N_B. \tag{84}$$

Substituting Eq. (51) into Eqs. (9)–(11), we get the principal moments of inertia for a center-ringed planar star,

$$I_1 \equiv mL^2 \left(-1 + \sum_{c=1}^{c=N_B} c^2 \right) \sum_{n=1}^{n=N_A} \sin^2 \left[(n-1) \frac{2\pi}{N_A} \right] \equiv mL^2 (-1 + Z)\alpha, \tag{85}$$

$$I_2 \equiv mL^2 \left(-1 + \sum_{c=1}^{c=N_B} c^2 \right) \sum_{n=1}^{n=N_A} \cos^2 \left[(n-1) \frac{2\pi}{N_A} \right] \equiv mL^2 (-1 + Z)\beta, \tag{86}$$

$$I_3 \equiv 2mL^2 \left(-1 + \sum_{c=1}^{c=N_B} c^2 \right) \sum_{n=1}^{n=N_A} \cos^2 \left[(n-1) \frac{2\pi}{N_A} \right] \equiv 2mL^2 (-1 + Z)\beta. \tag{87}$$

Substituting Eqs. (59)–(61) into Eqs. (85) gives

$$I_1 \equiv mL^2 [-1 + N_B(N_B + 1)(2N_B + 1)] \frac{N_A}{2}, \tag{88}$$

$$I_2 \equiv mL^2 [-1 + N_B(N_B + 1)(2N_B + 1)] \frac{N_A}{2} = I_1, \tag{89}$$

$$I_3 \equiv mL^2 [-1 + N_B(N_B + 1)(2N_B + 1)] N_A. \tag{90}$$

Substituting Eqs. (88)–(90) into Eqs. (16)–(18) gives the orientation constants for a center-ringed planar star-branched polymer,

$$a \equiv \frac{7}{30} [-1 + N_B(N_B + 1)(2N_B + 1)] N_A, \tag{91}$$

$$b \equiv \frac{3}{5}, \tag{92}$$

$$\nu \equiv \frac{12}{[-1 + N_B(N_B + 1)(2N_B + 1)] N_A}. \tag{93}$$

Multiplying a by ν gives

$$a\nu = \frac{14}{5}, \tag{94}$$

as it must, for $b = 3/5$ (see Fig. 3 of Ref. 1). Inserting Eq. (93) into Eq. (26) yields

$$\frac{\lambda}{\lambda_0} \equiv N_A [-1 + N_B(N_B + 1)(2N_B + 1)], \tag{95}$$

for center-ringed stars with $3 \leq N_A \leq 6$.

Equations (91)–(93) are subject to Eq. (21). To check consistency, we substitute Eqs. (88) and (90) into Eq. (21) and get

$$\frac{1}{4} < \frac{5}{6}, \tag{96}$$

as it should, for all center-ringed planar stars.

We next examine the special case of the N -bead star-branched polymer, with single-beaded arms ($N_A = N, N_B = 1$),

$$a \equiv \frac{7}{6}N, \tag{97}$$

and

$$\nu \equiv \frac{12}{5N}, \tag{98}$$

which match row 3 of Table I (or row 3 of Table XV of Ref. 1) as they must.

Substituting Eqs. (91)–(93) into Eqs. (44) and (35)

$$\frac{\eta'}{nkT\lambda_0} = \frac{7}{5}[-1 + N_B(N_B + 1)(2N_B + 1)]N_A \left\{ 1 + \frac{3}{7} \left(\frac{1}{1 + (\lambda\omega)^2} \right) \right\}, \tag{99}$$

$$\frac{\eta''}{nkT\lambda_0} = \frac{3}{5}[-1 + N_B(N_B + 1)(2N_B + 1)]N_A \left\{ \frac{1}{1 + (\lambda\omega)^2} \right\}, \tag{100}$$

as $\lambda\omega \rightarrow 0$,

$$\frac{\eta_0}{nkT\lambda_0} = 2[-1 + N_B(N_B + 1)(2N_B + 1)]N_A, \tag{101}$$

resulting in the same equations for η'/η_0 and η''/η_0 for center-ringed when $N_A \leq 6$ as center-beaded when $3 \leq N_A \leq 6$ [Eqs. (80) and (81)], illustrated in Figs. 6 and 7.

To deepen our understanding of how branching affects the rheology of center-ringed planar stars ($3 \leq N_A \leq 6$), we can normalize our main result, Eq. (101), with Eq. (47),

$$\frac{n^\ell \eta_0}{m\eta_0^\ell} = \frac{12(N_B + 1)(2N_B + 1)}{(N_A N_B + 1)(N_A N_B + 2)} - \frac{12}{N_B(N_A N_B + 1)(N_A N_B + 2)}, \tag{102}$$

and Eq. (69), with Eq. (4),

$$\frac{\lambda}{\lambda^\ell} = \frac{6(N_B + 1)(2N_B + 1)}{(N_A N_B + 1)(N_A N_B + 2)} - \frac{6}{N_B(N_A N_B + 1)(N_A N_B + 2)}, \tag{103}$$

where the superscripted ℓ indicates unbranched.

C. Center-beaded planar stars ($N_A \geq 7$)

For center-beaded planar stars, Eqs. (54) and (52) are subject to Eqs. (53) and (55).

Substituting Eq. (54) into Eqs. (9)–(11), we get the principal moments of inertia for a center-beaded planar star,

$$I_1 \equiv mL^2 \sum_{c=1}^{c=N_B} c^2 \sum_{n=1}^{n=N_A} \frac{\sin^2 \left[(n-1) \frac{2\pi}{N_A} \right]}{4 \sin^2 \left(\frac{\pi}{N_A} \right)} \equiv mL^2 Z\alpha_c, \tag{104}$$

$$I_2 \equiv mL^2 \sum_{c=1}^{c=N_B} c^2 \sum_{n=1}^{n=N_A} \frac{\cos^2 \left[(n-1) \frac{2\pi}{N_A} \right]}{4 \sin^2 \left(\frac{\pi}{N_A} \right)} \equiv mL^2 Z\beta_c, \tag{105}$$

$$I_3 \equiv 2mL^2 \sum_{c=1}^{c=N_B} c^2 \sum_{n=1}^{n=N_A} \frac{\cos^2 \left[(n-1) \frac{2\pi}{N_A} \right]}{4 \sin^2 \left(\frac{\pi}{N_A} \right)} \equiv 2mL^2 Z\beta_c. \tag{106}$$

From Eq. (59) and Eqs. (106)–(108), we get

$$\begin{aligned} \alpha_c &\equiv \sum_{n=1}^{n=N_A} \frac{\sin^2 \theta_n}{4 \sin^2 \frac{\pi}{N_A}} = \sum_{n=1}^{n=N_A} \sin^2 \left[(n-1) \frac{2\pi}{N_A} \right] \sum_{n=1}^{n=N_A} \frac{1}{4 \sin^2 \frac{\pi}{N_A}} \\ &= \frac{N_A}{8 \sin^2 \frac{\pi}{N_A}}, \end{aligned} \tag{107}$$

$$\begin{aligned} \beta_c &\equiv \sum_{n=1}^{n=N_A} \frac{\cos^2 \theta_n}{4 \sin^2 \frac{\pi}{N_A}} = \sum_{n=1}^{n=N_A} \cos^2 \left[(n-1) \frac{2\pi}{N_A} \right] \sum_{n=1}^{n=N_A} \frac{1}{4 \sin^2 \left(\frac{\pi}{N_A} \right)} \\ &= \frac{N_A}{8 \sin^2 \frac{\pi}{N_A}} = \alpha_c. \end{aligned} \tag{108}$$

Substituting Eqs. (59) and (107) into Eq. (104) gives

$$I_1 \equiv \frac{N_A}{8 \sin^2 \frac{\pi}{N_A}} N_B(N_B + 1)(2N_B + 1)mL^2, \tag{109}$$

and Eqs. (59) and (108) into Eq. (105),

$$I_2 \equiv \frac{N_A}{8 \sin^2 \frac{\pi}{N_A}} N_B(N_B + 1)(2N_B + 1)mL^2 = I_1, \tag{110}$$

and Eqs. (59) and (108) into Eq. (106),

$$I_3 \equiv \frac{N_A}{4 \sin^2 \frac{\pi}{N_A}} N_B(N_B + 1)(2N_B + 1)mL^2. \tag{111}$$

Substituting Eqs. (109)–(111) into Eqs. (16)–(18) gives the orientation constants for a center-beaded planar star-branched polymer,

$$a \equiv \frac{7}{120 \sin^2 \frac{\pi}{N_A}} N_A N_B(N_B + 1)(2N_B + 1), \tag{112}$$

$$b \equiv \frac{3}{5}, \tag{113}$$

$$\nu \equiv \frac{48 \sin^2 \frac{\pi}{N_A}}{N_A N_B(N_B + 1)(2N_B + 1)}, \tag{114}$$

which match row 4 of Table I (or row 4 of Table XV of Ref. 1) as they must.

Multiplying a by ν gives

$$a\nu = \frac{14}{5}, \tag{115}$$

as it must, for $b = 3/5$ (see Fig. 3 of Ref. 1). Inserting Eq. (114) into Eq. (26) yields

$$\frac{\lambda}{\lambda_0} \equiv \frac{N_A N_B(N_B + 1)(2N_B + 1)}{4 \sin^2 \frac{\pi}{N_A}}, \tag{116}$$

for center-beaded stars with $N_A \geq 7$.

Equations (112)–(114) are subject to Eq. (21). Substituting Eqs. (109) and (111) into Eq. (21) gives, for all center-beaded planar stars,

$$\frac{1}{4} < \frac{5}{6}, \tag{117}$$

as it should.

Substituting Eqs. (112)–(114) into Eqs. (44) and (35),

$$\frac{\eta'}{nkT\lambda_0} = \frac{7}{20 \sin^2 \frac{\pi}{N_A}} N_A N_B (N_B + 1) (2N_B + 1) \left\{ 1 + \frac{3}{7} \left(\frac{1}{1 + (\lambda\omega)^2} \right) \right\}, \tag{118}$$

$$\frac{\eta''}{nkT\lambda_0} = \frac{3}{20 \sin^2 \frac{\pi}{N_A}} N_A N_B (N_B + 1) (2N_B + 1) \left\{ \frac{1}{1 + (\lambda\omega)^2} \right\}, \tag{119}$$

as $\lambda\omega \rightarrow 0$,

$$\frac{\eta_0}{nkT\lambda_0} = \frac{1}{2 \sin^2 \frac{\pi}{N_A}} N_A N_B (N_B + 1) (2N_B + 1), \tag{120}$$

resulting in the same equations for η'/η_0 and η''/η_0 for center-beaded when $N_A \geq 7$ as center-beaded when $3 \leq N_A \leq 6$ [Eqs. (80) and (81)], illustrated in Figs. 6 and 7.

D. Center-ringed planar stars ($N_A \geq 7$)

For center-ringed planar stars, Eqs. (51) and (52) are subject to Eqs. (53) and (84). Substituting Eq. (51) into Eqs. (9)–(11), we get the principal moments of inertia for a center-ringed planar star,

$$I_1 \equiv mL^2 \left(-1 + \sum_{c=1}^{c=N_B} c^2 \right) \sum_{n=1}^{n=N_A} \frac{\sin^2 \left[(n-1) \frac{2\pi}{N_A} \right]}{4 \sin^2 \frac{\pi}{N_A}} \tag{121}$$

$$\equiv mL^2 (-1 + Z) \alpha_c,$$

$$I_2 \equiv mL^2 \left(-1 + \sum_{c=1}^{c=N_B} c^2 \right) \sum_{n=1}^{n=N_A} \frac{\cos^2 \left[(n-1) \frac{2\pi}{N_A} \right]}{4 \sin^2 \frac{\pi}{N_A}} \tag{122}$$

$$\equiv mL^2 (-1 + Z) \beta_c,$$

$$I_3 \equiv 2mL^2 \left[\left(-1 + \sum_{c=1}^{c=N_B} c^2 \right) \sum_{n=1}^{n=N_A} \frac{\cos^2 \left((n-1) \frac{2\pi}{N_A} \right)}{4 \sin^2 \frac{\pi}{N_A}} \right] \tag{123}$$

$$\equiv 2mL^2 (-1 + Z) \beta_c.$$

Substituting Eqs. (59), (107), and (108) into Eqs. (121)–(123) gives

$$I_1 \equiv mL^2 [-1 + N_B(N_B + 1)(2N_B + 1)] \frac{N_A}{8 \sin^2 \frac{\pi}{N_A}}, \tag{124}$$

$$I_2 \equiv mL^2 [-1 + N_B(N_B + 1)(2N_B + 1)] \frac{N_A}{8 \sin^2 \frac{\pi}{N_A}} = I_1, \tag{125}$$

$$I_3 \equiv mL^2 [-1 + N_B(N_B + 1)(2N_B + 1)] \frac{N_A}{4 \sin^2 \frac{\pi}{N_A}}. \tag{126}$$

Substituting Eqs. (124)–(126) into Eqs. (16)–(18) gives the orientation constants for a center-ringed planar star-branched polymer,

$$a \equiv \frac{7}{120 \sin^2 \frac{\pi}{N_A}} [-1 + N_B(N_B + 1)(2N_B + 1)] N_A, \tag{127}$$

$$b \equiv \frac{3}{5}, \tag{128}$$

$$\nu \equiv \frac{48 \sin^2 \frac{\pi}{N_A}}{(-1 + N_B(N_B + 1)(2N_B + 1)) N_A}, \tag{129}$$

as it must, for $b = 3/5$ (see Fig. 3 of Ref. 1) which match row 4 of Table I (or row 4 of Table XV of Ref. 1) as they must. Inserting Eq. (129) into Eq. (26) yields

$$\frac{\lambda}{\lambda_0} \equiv \frac{[-1 + N_B(N_B + 1)(2N_B + 1)] N_A}{4 \sin^2 \frac{\pi}{N_A}} \tag{130}$$

for center-beaded stars with $N_A > 7$.

Equations (127)–(129) are subject to Eq. (21). Substituting Eqs. (127)–(129) into Eq. (21) gives, for all center-ringed planar stars,

$$\frac{1}{4} < \frac{5}{6}, \tag{131}$$

as it should.

Substituting Eqs. (127)–(129) into Eqs. (44) and (35),

$$\frac{\eta'}{nkT\lambda_0} = \frac{7}{20 \sin^2 \frac{\pi}{N_A}} [-1 + N_B(N_B + 1)(2N_B + 1)] N_A \times \left\{ 1 + \frac{3}{7} \left(\frac{1}{1 + (\lambda\omega)^2} \right) \right\}, \tag{132}$$

$$\frac{\eta''}{nkT\lambda_0} = \frac{3}{20 \sin^2 \frac{\pi}{N_A}} [-1 + N_B(N_B + 1)(2N_B + 1)] N_A \left\{ \frac{1}{1 + (\lambda\omega)^2} \right\}, \tag{133}$$

as $\lambda\omega \rightarrow 0$,

$$\frac{\eta_0}{nkT\lambda_0} = \frac{1}{2 \sin^2 \frac{\pi}{N_A}} [-1 + N_B(N_B + 1)(2N_B + 1)] N_A, \tag{134}$$

resulting in the same equations for η'/η_0 and η''/η_0 for center-ringed when $N_A \geq 7$ as center-beaded when $3 \leq N_A \leq 6$ [Eqs. (80) and (81)], illustrated in Figs. 6 and 7.

IV. RESULTS: TETRAHEDRAL STARS

In spherical coordinates, the bead positions for the irregular tetrahedra between osculated and planar are

$$\phi = 0, \pi, \frac{\pi}{2}, \frac{3\pi}{2}, \tag{135}$$

$$\theta = \theta_1, \theta_1, \pi - \theta_1, \pi - \theta_1, \tag{136}$$

where

$$\sin^{-1} \frac{d}{2L} \leq \theta_1 \leq \frac{\pi}{2} \tag{137}$$

or

$$\sin^{-1} \frac{d}{2L} \leq \theta_1 \leq 90^\circ, \tag{138}$$

where $\theta_1 = \frac{\pi}{2}$ is the planar 4-arm star, and where $\frac{1}{2}(\pi - \Theta_t) = 0.62$ rad corresponds to the regular tetrahedron (spherically symmetric). By *osculated*, we mean that θ_1 is such that the first beads on adjacent branches kiss. Here, $\Theta_t \equiv \cos^{-1}(-\frac{1}{3}) \cong \frac{\pi}{2} + \frac{2\sqrt{2}}{9} \cong 109.5^\circ$ and is the *tetrahedral angle* of organic chemistry.

A. Center-beaded tetrahedral stars ($N_A = 4$)

On the unit sphere,

$$\mathbf{R}_i = \begin{cases} (0, \theta, \phi), \\ (1, \theta_1, 0), \\ (1, \theta_1, \pi), \\ (1, \pi - \theta_1, \frac{\pi}{2}), \\ (1, \pi - \theta_1, \frac{3\pi}{2}), \end{cases} \quad (139)$$

defined by Fig. 8, where in Cartesian coordinates [Eqs. (A.6-19) through (A.6-21) of Ref. 20],

$$R_{i1} = \sin \theta \cos \phi, \quad (140)$$

$$R_{i2} = \sin \theta \sin \phi, \quad (141)$$

$$R_{i3} = \cos \theta, \quad (142)$$

which are subject to Eqs. (135) and (136), so that

$$\mathbf{R}_i = cL \begin{cases} (0, 0, 0), \\ (\sin \theta_1, 0, \cos \theta_1), \\ (-\sin \theta_1, 0, \cos \theta_1), \\ (0, \sin(\pi - \theta_1), \cos(\pi - \theta_1)), \\ (0, -\sin(\pi - \theta_1), \cos(\pi - \theta_1)), \end{cases} \quad (143)$$

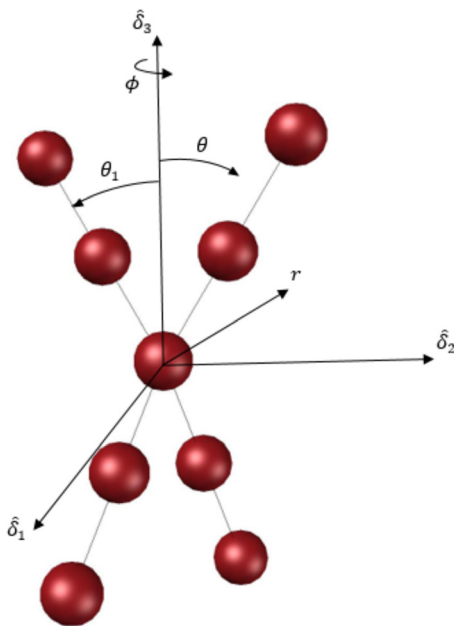


FIG. 8. Molecular coordinates installed on 4-arm star. Specific example of center-beaded regular tetrahedral star ($\theta_1 = \frac{1}{2}\theta_t$) with $N_B = 2$. Spherical coordinates follow Figs. (A.8)–(A.12) of Ref. 20.

which is subject to Eq. (137), and where $c = 1, 2, \dots, N_B$. Figures 9 and 10 illustrate these definitions.

Substituting Eq. (143) into Eqs. (9)–(11), we get the principal moments of inertia for a center-beaded irregular tetrahedral star,

$$I_1 = 2mL^2 [1 + 2 \cos^2 \theta_1] N_B(N_B + 1)(2N_B + 1), \quad (144)$$

$$I_2 = 2mL^2 [1 + 2 \cos^2 \theta_1] N_B(N_B + 1)(2N_B + 1) = I_1, \quad (145)$$

$$I_3 = 4mL^2 \sin^2 \theta_1 N_B(N_B + 1)(2N_B + 1). \quad (146)$$

Substituting Eqs. (144) and (146) into Eqs. (16)–(18) gives the orientation constants for a center-beaded tetrahedral star-branched polymer,

$$a \equiv \frac{N_B(N_B + 1)(2N_B + 1)}{15(\cos 2\theta_1 + 3)} [2 \cos 2\theta_1 - 5 \cos 4\theta_1 + 35], \quad (147)$$

$$b \equiv \frac{3(3 \cos^2 \theta_1 - 1)^2}{5(\cos^2 \theta_1 + 1)^2} = \frac{3(3 \cos 2\theta_1 + 1)^2}{5(\cos 2\theta_1 + 3)^2}, \quad (148)$$

$$\nu \equiv \frac{3}{[\cos 2\theta_1 + 2] N_B(N_B + 1)(2N_B + 1)}, \quad (149)$$

where

$$\frac{b}{\nu} = \frac{3(3 \cos 2\theta_1 + 1)^2 [\cos 2\theta_1 + 2] N_B(N_B + 1)(2N_B + 1)}{15(\cos 2\theta_1 + 3)^2}. \quad (150)$$

Since $a < 0$ is unphysical, from Eq. (147), we learn that

$$2 \cos 2\theta_1 - 5 \cos 4\theta_1 + 35 > 0, \quad (151)$$

which is always satisfied.

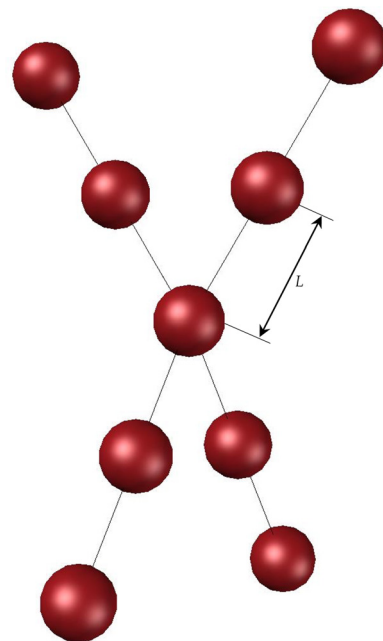


FIG. 9. Defining L for center-beaded regular tetrahedral star-branched macromolecule. Specific example: $N_A = 4$, $N_B = 2$. \mathbf{R}_i given by Eq. (143) with $\theta_1 = \frac{1}{2}(\pi - \theta_t)$ and $c = 1, \dots, N_B$.

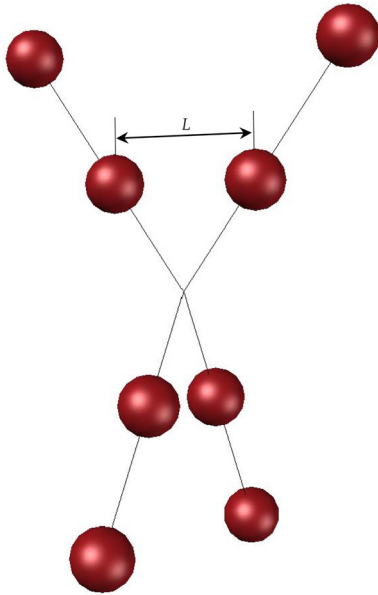


FIG. 10. Bead location for determining L for coreless regular tetrahedral star-branched macromolecule. Specific example: $N_A = 4$, $N_B = 2$. R_i given by Eq. (143) with $\theta_1 = \frac{1}{2}\theta_t$ and $c = 1, \dots, N_B$.

Multiplying a by ν gives

$$a\nu = \frac{2 \cos 2\theta_1 - 5 \cos 4\theta_1 + 35}{5(\cos 2\theta_1 + 3)[\cos 2\theta_1 + 2]}, \quad (152)$$

which, mindful of Eqs. (148) and (137), is a parametric function of b in θ_1 (see Fig. 3 of Ref. 1). Figure 11 illustrates, with Eqs. (152) and (148), how the macromolecular lopsidedness evolves with θ_1 . Figure 12 shows the progression in the $a\nu - b$ plane of the tetrahedral structures, starting with planar 4-arm stars (rightmost point on upper oblate branch) and progression leftward as θ_1 descends from $\frac{\pi}{2}$. From Fig. 12, we discover that at $\theta_1 = \frac{1}{2}\theta_t$ the leftward progression jumps to the lower prolate branch, ending at

$$b = \frac{3(3 \cos(\pi - \Theta_t) + 1)^2}{5(\cos(\pi - \Theta_t) + 3)^2}, \quad (153)$$

where $\theta_1 = \frac{1}{2}(\pi - \Theta_t)$, and where the 4-arm star is regular tetrahedral. Thus

$$\frac{3(3 \cos(\pi - \Theta_t) + 1)^2}{5(\cos(\pi - \Theta_t) + 3)^2} \leq b \leq \frac{3}{5}, \quad (154)$$

for tetrahedral macromolecules. When Eqs. (144) and (146) equate ($I_1 = I_3$), this gives

$$\theta_1 = \frac{\pi}{3}, \quad (155)$$

from which we learn that prolate tetrahedral macromolecules, from Eq. (137), range from

$$\sin^{-1} \frac{d}{2L} \leq \theta_1 < \frac{\pi}{3}, \quad (156)$$

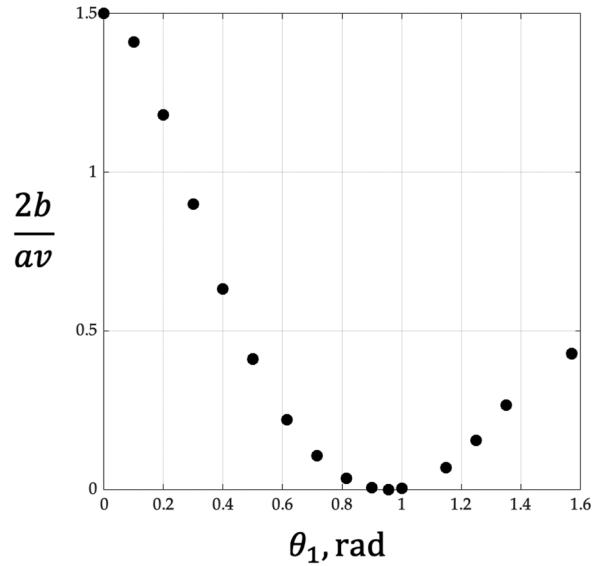


FIG. 11. $2b/av$ vs θ_1 for tetrahedral macromolecules, both regular and irregular. $a\nu$ and b , given by Eqs. (152) and (148) [Eqs. (22) and (23) of Ref. 1] are parametric in θ_1 over the range Eq. (137). The interior angle of the tetrahedra decreases with θ_1 .

and oblate

$$\frac{\pi}{3} < \theta_1 \leq \frac{\pi}{2}, \quad (157)$$

illustrated in Fig. 12 (and Figs. 3 and 17 of Ref. 1).

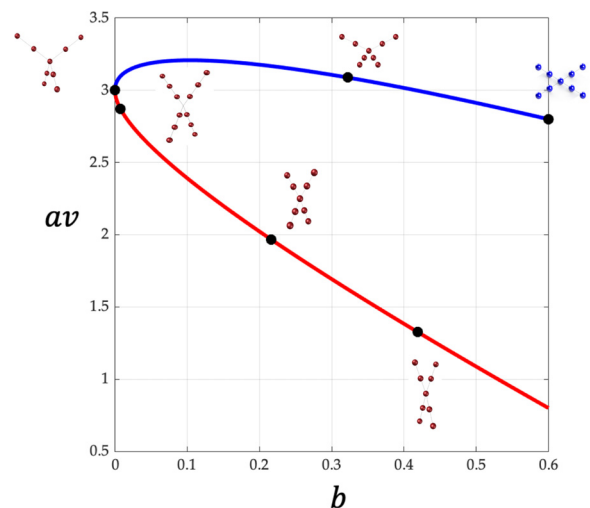


FIG. 12. $a\nu$ vs b for tetrahedral macromolecules, both regular and irregular. $a\nu$ and b , given by Eqs. (152) and (148) [Eqs. (22) and (23) of Ref. 1] are parametric in θ_1 over the range Eq. (137). The oblate branch (top, right to left) has macromolecules of $\theta_1 = \frac{\pi}{2}$ rad and 1.3 rad and for the prolate branch (bottom, left to right) has macromolecules of $\theta_1 = \frac{\Theta_t}{2}$, $\theta_1 = 0.90$, $\theta_1 = \frac{1}{2}(\pi - \Theta_t)$, and $\theta_1 = 0.40$ rad.

Inserting Eq. (149) into Eq. (26) yields

$$\frac{\lambda}{\lambda_0} \equiv 4[\cos 2\theta_1 + 2]N_B(N_B + 1)(2N_B + 1), \quad (158)$$

for center-beaded tetrahedral stars.

Equations (147)–(149) are subject to Eq. (21). Substituting Eqs. (147)–(149) into Eqs. (40) and (41) yields, for suspensions of center-beaded tetrahedral star-branched polymers,

$$\frac{\eta' - \eta_s}{\eta_0 - \eta_s} = \frac{1 + \frac{6(3 \cos 2\theta_1 + 1)^2 [\cos 2\theta_1 + 2]}{[2 \cos 2\theta_1 - 5 \cos 4\theta_1 + 35](\cos 2\theta_1 + 3)} \left(\frac{1}{1 + (\lambda\omega)^2} \right)}{1 + \frac{6(3 \cos 2\theta_1 + 1)^2 [\cos 2\theta_1 + 2]}{[2 \cos 2\theta_1 - 5 \cos 4\theta_1 + 35](\cos 2\theta_1 + 3)}} \quad (159)$$

and

$$\frac{\eta''}{\eta_0 - \eta_s} = \frac{6(3 \cos 2\theta_1 + 1)^2 [\cos 2\theta_1 + 2]}{[2 \cos 2\theta_1 - 5 \cos 4\theta_1 + 35](\cos 2\theta_1 + 3)} \left\{ \frac{\lambda\omega}{1 + (\lambda\omega)^2} \right\}, \quad (160)$$

which we will recover, from time to time, below.

Substituting Eqs. (147)–(149) into Eqs. (44) and (35),

$$\begin{aligned} \frac{\eta'}{nkT\lambda_0} &= 6 \frac{N_B(N_B + 1)(2N_B + 1)}{15(\cos 2\theta_1 + 3)} [2 \cos 2\theta_1 - 5 \cos 4\theta_1 + 35] \\ &\times \left\{ 1 + \frac{6[\cos 2\theta_1 + 2](3 \cos 2\theta_1 + 1)^2}{(\cos 2\theta_1 + 3)[2 \cos 2\theta_1 - 5 \cos 4\theta_1 + 35]} \right. \\ &\times \left. \left(\frac{1}{1 + (\lambda\omega)^2} \right) \right\} \end{aligned} \quad (161)$$

and

$$\begin{aligned} \frac{\eta''}{nkT\lambda_0} &= 6 \frac{N_B(N_B + 1)(2N_B + 1)}{15(\cos 2\theta_1 + 3)} [2 \cos 2\theta_1 - 5 \cos 4\theta_1 + 35] \\ &\times \left\{ \frac{6[\cos 2\theta_1 + 2](3 \cos 2\theta_1 + 1)^2}{(\cos 2\theta_1 + 3)[2 \cos 2\theta_1 - 5 \cos 4\theta_1 + 35]} \frac{\lambda\omega}{1 + (\lambda\omega)^2} \right\} \end{aligned} \quad (162)$$

as $\lambda\omega \rightarrow 0$,

$$\begin{aligned} \frac{\eta_0}{nkT\lambda_0} &= 6 \frac{N_B(N_B + 1)(2N_B + 1)}{15(\cos 2\theta_1 + 3)} [2 \cos 2\theta_1 - 5 \cos 4\theta_1 + 35] \\ &\times \left\{ 1 + \frac{6[\cos 2\theta_1 + 2](3 \cos 2\theta_1 + 1)^2}{(\cos 2\theta_1 + 3)[2 \cos 2\theta_1 - 5 \cos 4\theta_1 + 35]} \right\}, \end{aligned} \quad (163)$$

which we illustrate in Fig. 13. We find the behavior of Fig. 13 to be intrinsically beautiful. Normalizing Eqs. (161) and (162) with Eq. (163) gives

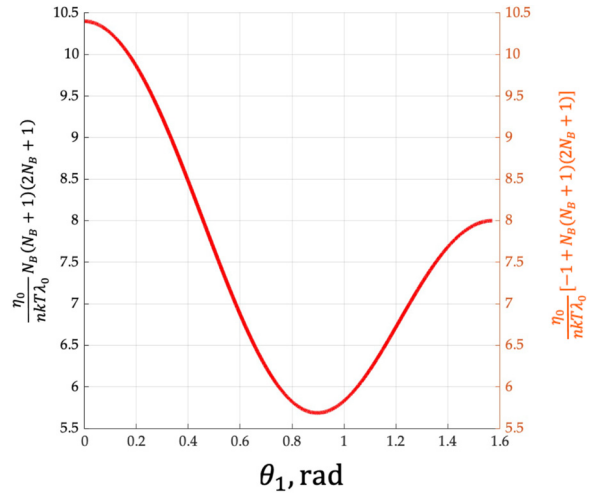


FIG. 13. $N_B(N_B + 1)(2N_B + 1)\eta_0/nkT\lambda_0$ and $[-1 + N_B(N_B + 1)(2N_B + 1)]\eta_0/nkT\lambda_0$ vs θ_1 from Eqs. (163) and (178) for center-beaded and coreless tetrahedral stars.

$$\frac{\eta'}{\eta_0} = \frac{1 + \frac{6[\cos 2\theta_1 + 2](3 \cos 2\theta_1 + 1)^2}{(\cos 2\theta_1 + 3)[2 \cos 2\theta_1 - 5 \cos 4\theta_1 + 35]} \left(\frac{1}{1 + (\lambda\omega)^2} \right)}{1 + \frac{6[\cos 2\theta_1 + 2](3 \cos 2\theta_1 + 1)^2}{(\cos 2\theta_1 + 3)[2 \cos 2\theta_1 - 5 \cos 4\theta_1 + 35]}} \quad (164)$$

and

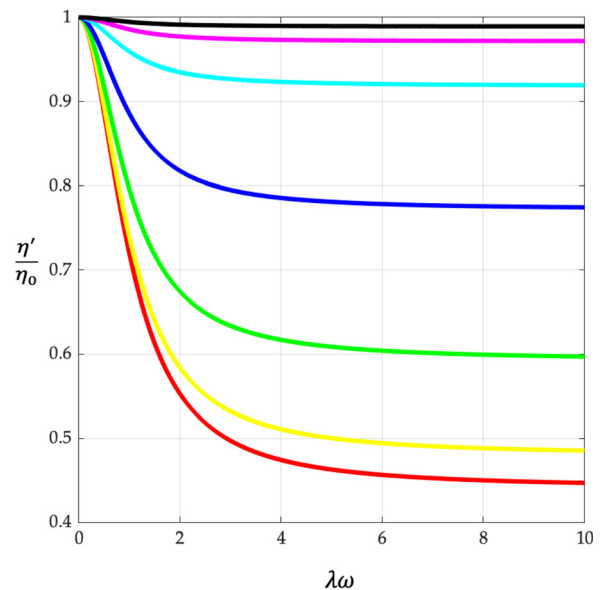


FIG. 14. $\eta'/\eta_0(\lambda\omega)$ from Eq. (164) for center-beaded and coreless tetrahedral stars at varying θ_1 for prolate macromolecules [Eq. (156)] [black: $\theta_1 = \frac{1}{2}\Theta_i$; magenta: $\theta_1 = 0.90$ rad; cyan: $\theta_1 = 0.80$ rad; blue: $\theta_1 = \frac{1}{2}(\pi - \Theta_i)$ rad; green: $\theta_1 = 0.40$ rad; yellow: $\theta_1 = 0.20$ rad; red: $\theta_1 = 0.0$ rad].

$$\frac{\eta''}{\eta_0} = \frac{6[\cos 2\theta_1 + 2](3 \cos 2\theta_1 + 1)^2}{(\cos 2\theta_1 + 3)[2 \cos 2\theta_1 - 5 \cos 4\theta_1 + 35]} \frac{\lambda\omega}{1 + (\lambda\omega)^2} \quad (165)$$

We illustrate Eq. (164) for η' in Figs. 14 (prolate) and 15 (oblate), and Eq. (165) for η'' in Figs. 16 (prolate) and 17 (oblate). From Eq. (164), we then learn that for tetrahedral center-beaded star suspensions, from general rigid bead-rod theory, opening the interior angle of the tetrahedron decreases the real part of the complex viscosity. From Eq. (165), we then learn that for tetrahedral center-beaded star suspensions, from general rigid bead-rod theory, opening the interior angle of the tetrahedron increases the imaginary part of the complex viscosity.

To deepen our understanding of how branching affects the rheology of center-beaded tetrahedral stars ($N_A = 4$), we can normalize our main result, Eq. (163), with Eq. (47),

$$\frac{n^\ell \eta_0}{m \eta_0^\ell} = \frac{72 N_B (N_B + 1) (2 N_B + 1)}{N_A N_B (N_A N_B + 1) (N_A N_B + 2)} \times \left\{ \frac{[\cos 2\theta_1 + 2](3 \cos 2\theta_1 + 1)^2 + (\cos 2\theta_1 + 3)[2 \cos 2\theta_1 - 5 \cos 4\theta_1 + 35]}{5(\cos 2\theta_1 + 3)^2} \right\}, \quad (166)$$

and Eq. (158) with Eq. (4),

$$\frac{\lambda}{\lambda^\ell} = \frac{24[\cos 2\theta_1 + 2] N_B (N_B + 1) (2 N_B + 1)}{N_A N_B (N_A N_B + 1) (N_A N_B + 2)}, \quad (167)$$

where the superscripted ℓ indicates unbranched.

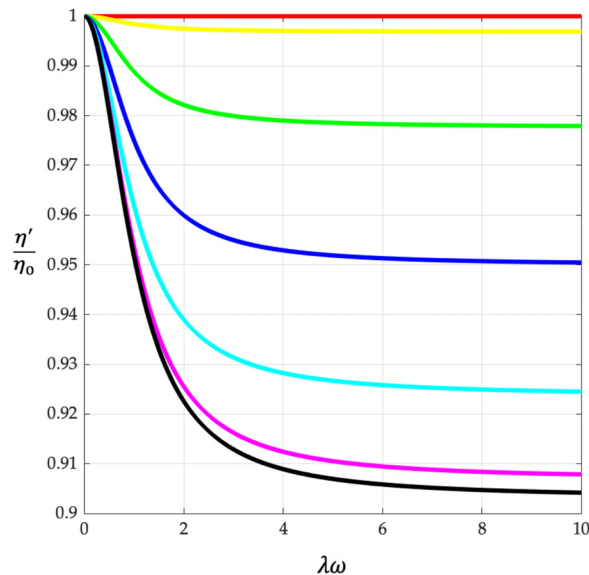


FIG. 15. $\eta'/\eta_0(\lambda\omega)$ from Eq. (164) for center-beaded and coreless tetrahedral stars at varying θ_1 for oblate macromolecules [Eq. (157)] [black: $\theta_1 = \frac{1}{2}\pi$; magenta: $\theta_1 = 1.5$ rad; cyan: $\theta_1 = 1.4$ rad; blue: $\theta_1 = 1.3$ rad; green: $\theta_1 = 1.2$ rad; yellow: $\theta_1 = 1.1$ rad; red: $\theta_1 = \frac{1}{3}\pi$].

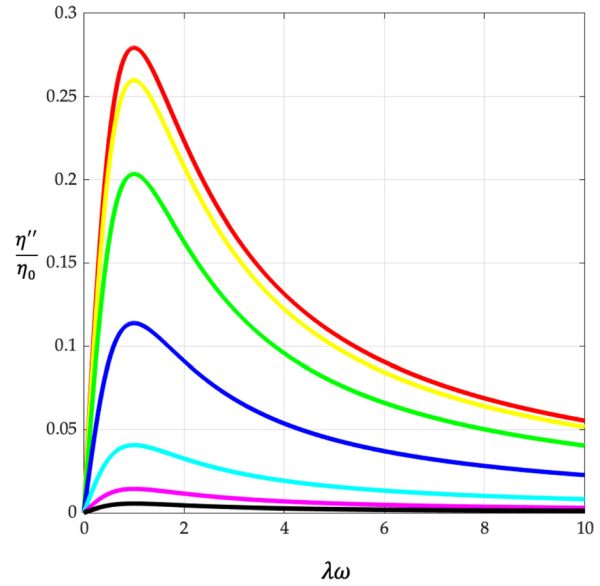


FIG. 16. $\eta''/\eta_0(\lambda\omega)$ from Eq. (166) for center-beaded and coreless tetrahedral stars at varying θ_1 for prolate macromolecules [Eq. (156)] [black: $\theta_1 = \frac{1}{2}\Theta$; magenta: $\theta_1 = 0.90$ rad; cyan: $\theta_1 = 0.80$ rad; blue: $\theta_1 = \frac{1}{2}(\pi - \Theta)$ rad; green: $\theta_1 = 0.40$ rad; yellow: $\theta_1 = 0.20$ rad; red: $\theta_1 = 0.0$ rad].

B. Coreless tetrahedral stars ($N_A = 4$)

For coreless tetrahedral stars, Eq. (143) is subject to Eq. (84). Substituting Eq. (143) into Eqs. (9)–(11), we get the principal moments of inertia for a coreless irregular tetrahedral star,

$$I_1 = 2mL^2 [1 + 2 \cos^2 \theta_1] [-1 + N_B(N_B + 1)(2N_B + 1)], \quad (168)$$

$$I_2 = 2mL^2 [1 + 2 \cos^2 \theta_1] [-1 + N_B(N_B + 1)(2N_B + 1)] = I_1, \quad (169)$$

$$I_3 = 4mL^2 \sin^2(\theta_1) [-1 + N_B(N_B + 1)(2N_B + 1)], \quad (170)$$

by *coreless*, we mean, the macromolecule lacks a center bead. Substituting Eqs. (168)–(170) into Eqs. (16)–(18) gives the orientation constants for a coreless tetrahedral star-branched polymer,

$$a \equiv \frac{[-1 + N_B(N_B + 1)(2N_B + 1)]}{15(\cos 2\theta_1 + 3)} [2 \cos 2\theta_1 - 5 \cos 4\theta_1 + 35], \quad (171)$$

$$b \equiv \frac{3(3 \cos 2\theta_1 + 1)^2}{5(\cos 2\theta_1 + 3)^2}, \quad (172)$$

$$\nu \equiv \frac{3}{[\cos 2\theta_1 + 2] [-1 + N_B(N_B + 1)(2N_B + 1)]}. \quad (173)$$

Multiplying a by ν gives at $\theta_1 = \pi/2$,

$$a\nu = \frac{14}{5}, \quad (174)$$

as it must, for $b = 3/5$ (see Fig. 3 of Ref. 1). Inserting Eq. (173) into Eq. (26) yields

$$\frac{\lambda}{\lambda_0} \equiv 4[\cos 2\theta_1 + 2] [-1 + N_B(N_B + 1)(2N_B + 1)], \quad (175)$$

for coreless tetrahedral stars.

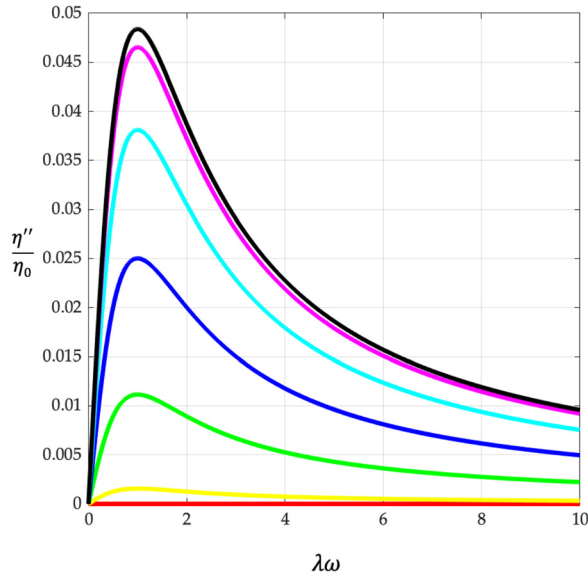


FIG. 17. $\eta''/\eta_0(\lambda\omega)$ from Eq. (165) for center-beaded and coreless tetrahedral stars at varying θ_1 for oblate macromolecules [Eq. (157)] [black: $\theta_1 = \frac{1}{2}\pi$; magenta: $\theta_1 = 1.5$ rad; cyan: $\theta_1 = 1.4$ rad; blue: $\theta_1 = 1.3$ rad; green: $\theta_1 = 1.2$ rad; yellow: $\theta_1 = 1.1$ rad; red: $\theta_1 = \frac{1}{3}\pi$].

Equations (171)–(173) are subject to Eq. (21). Substituting Eqs. (171)–(173) into Eqs. (40) and (41) yields, for suspensions of coreless tetrahedral star-branched polymers resulting in the same equations for $(\eta' - \eta_s)/(\eta_0 - \eta_s)$ and $\eta''/(\eta_0 - \eta_s)$ [Eqs. (159) and (160)] as center-beaded tetrahedral stars.

Substituting Eqs. (171)–(173) into Eqs. (44) and (35),

$$\frac{\eta'}{nkT\lambda_0} = 6 \frac{[-1 + N_B(N_B + 1)(2N_B + 1)]}{15(\cos 2\theta_1 + 3)} [2 \cos 2\theta_1 - 5 \cos 4\theta_1 + 35] \times \left\{ 1 + \frac{6[\cos 2\theta_1 + 2](3 \cos 2\theta_1 + 1)^2}{(\cos 2\theta_1 + 3)[2 \cos 2\theta_1 - 5 \cos 4\theta_1 + 35]} \times \left(\frac{1}{1 + (\lambda\omega)^2} \right) \right\} \quad (176)$$

and

$$\frac{\eta''}{nkT\lambda_0} = 6 \frac{[-1 + N_B(N_B + 1)(2N_B + 1)]}{15(\cos 2\theta_1 + 3)} [2 \cos 2\theta_1 - 5 \cos 4\theta_1 + 35] \times \left\{ \frac{6[\cos 2\theta_1 + 2](3 \cos 2\theta_1 + 1)^2}{(\cos 2\theta_1 + 3)[2 \cos 2\theta_1 - 5 \cos 4\theta_1 + 35]} \frac{\lambda\omega}{1 + (\lambda\omega)^2} \right\}, \quad (177)$$

as $\lambda\omega \rightarrow 0$,

$$\frac{\eta_0}{nkT\lambda_0} = 6 \frac{[-1 + N_B(N_B + 1)(2N_B + 1)]}{15(\cos 2\theta_1 + 3)} [2 \cos 2\theta_1 - 5 \cos 4\theta_1 + 35] \times \left\{ 1 + \frac{6[\cos 2\theta_1 + 2](3 \cos 2\theta_1 + 1)^2}{(\cos 2\theta_1 + 3)[2 \cos 2\theta_1 - 5 \cos 4\theta_1 + 35]} \right\}, \quad (178)$$

illustrated in Fig. 13. Normalizing Eqs. (176) and (177) with Eq. (178) results in the same equations for η'/η_0 and η''/η_0 for center-beaded tetrahedral stars [Eqs. (164) and (165)], illustrated in Figs. 14 (prolate) and 15 (oblate) for η' , and in Figs. 16 (prolate) and 17 (oblate) for η'' .

To deepen our understanding of how branching affects the rheology of coreless tetrahedral stars ($N_A = 4$), we can normalize our main result, Eq. (163), with Eq. (47),

$$\frac{n^\ell \eta_0}{m \eta_0^\ell} = \frac{72[-1 + N_B(N_B + 1)(2N_B + 1)]}{N_A N_B (N_A N_B + 1)(N_A N_B + 2)} \times \left\{ \frac{[\cos 2\theta_1 + 2](3 \cos 2\theta_1 + 1)^2 + (\cos 2\theta_1 + 3)[2 \cos 2\theta_1 - 5 \cos 4\theta_1 + 35]}{5(\cos 2\theta_1 + 3)^2} \right\}, \quad (179)$$

and Eq. (158) with Eq. (4),

$$\frac{\lambda}{\lambda^\ell} = \frac{24[\cos(2\theta_1) + 2][-1 + N_B(N_B + 1)(2N_B + 1)]}{N_A N_B (N_A N_B + 1)(N_A N_B + 2)}, \quad (180)$$

where the superscripted ℓ indicates unbranched.

V. WORKED EXAMPLE: POLYBUTADIENE ($N_A = 4$)

In Subsections VA–VD of this worked example, we will test our main results for star-branched polymers by normalizing them with the well-known result for straight chains. We compare 4-arm star-branched polybutadiene macromolecules with their linear counterparts of the same molecular weight, 200 000 g/gmol. Each arm of our 4-arm stars thus has a molecular weight of 50 000 g/gmol. Since our polybutadiene synthesis was lithium initiated,³ our chains consist of *cis*, *trans*, and vinyl microstructures in significant proportions (see Row 1 of Table 9 of Ref. 23). Whereas *cis* and *trans* differ only by bond rotation, the vinyl segments have tacticity.²⁴ Further, the proportions of *cis* and *trans* vary only slightly with molecular weight (see

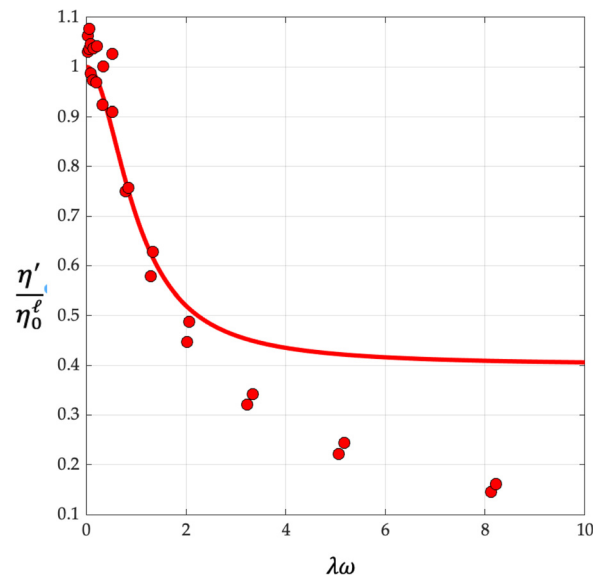


FIG. 18. η'/η_0^ℓ from Eq. (48) for unbranched fitted to data for straight chain in Ref. 9 ($\lambda = 0.2$ s, $\eta_0 = 2.55 \times 10^3$ Pa.s).



FIG. 19. Results for unbranched polybutadiene sample (PBA) explained with a four-bead shish-kebab.

Table I of Ref. 3). We rely specifically on the measurements of Ref. 9 on the 4-arm star (sample ST1, Fig. 7.10 of Ref. 9) and on the corresponding straight chain (sample PBA, Figs. 7.1, 7.2, 7.7, and 7.8 of Ref. 9) of nearly the same molecular weight and of nearly the same and narrow polydispersity. Figure 18 displays the fit of Eq. (1) to the measured values of complex viscosity of sample PBA (Figs. 7.2 and 7.3 of Ref. 9) and macromolecule illustrated in Fig. 19, yielding $\eta_0 = 2.55 \times 10^3$ Pa s and $\lambda = 0.20$ s for the straight chain.

Fitting Eq. (78) to the data from Fig. 7.10 of Ref. 9 yields Fig. 20, we get $\eta_0 = 1.27 \times 10^5$ Pa s and $\lambda = 54.0$ s for a center-beaded or center-ringed planar 4-arm star. Thus, we get (see Table IV)

$$\frac{n^\ell \eta_0}{n \eta_0^\ell} = 14.09 \tag{181}$$

from fitting general rigid bead-rod theory for center-beaded or center-ringed planar 4-arm star.

Fitting Eq. (164) to the data from Fig. 7.10 of Ref. 9, we get $\eta_0 = 1.38 \times 10^5$ Pa s, $\lambda = 57.0$ s, and $\theta_1 = 0.40$ rad for a center-

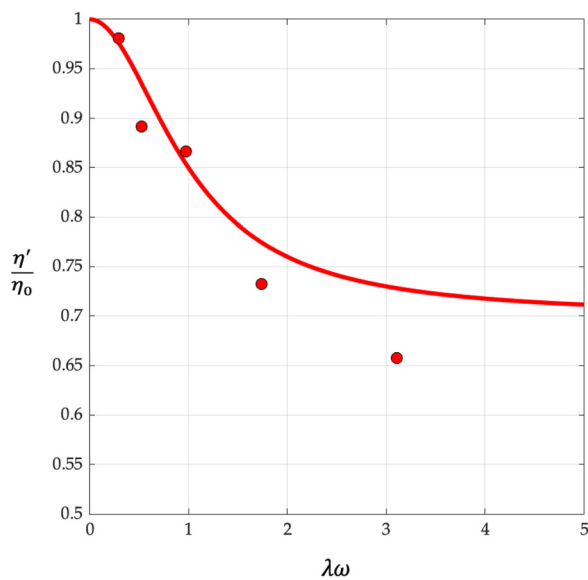


FIG. 20. $\eta'/\eta_0(\lambda\omega)$ from Eq. (78) for center-beaded and center-ringed planar star fitted to data for 4-arm star in Ref. 9 ($\eta_0 = 1.27 \times 10^5$ Pa s and $\lambda = 54.0$ s).

TABLE IV. Polybutadiene solution properties.

PBA	ST1—planar	ST1—tetrahedral
$\eta_0^\ell = 2.55 \times 10^3$ Pa s	$\eta_0 = 1.27 \times 10^5$ Pa s	$\eta_0 = 1.38 \times 10^5$ Pa s
$\lambda^\ell = 0.2$ s	$\lambda = 5.40 \times 10^1$ s	$\lambda = 5.70 \times 10^1$ s
$n^\ell = 0.0676$ g/cm ³	$n = 0.239$ g/cm ³	$n = 0.239$ g/cm ³

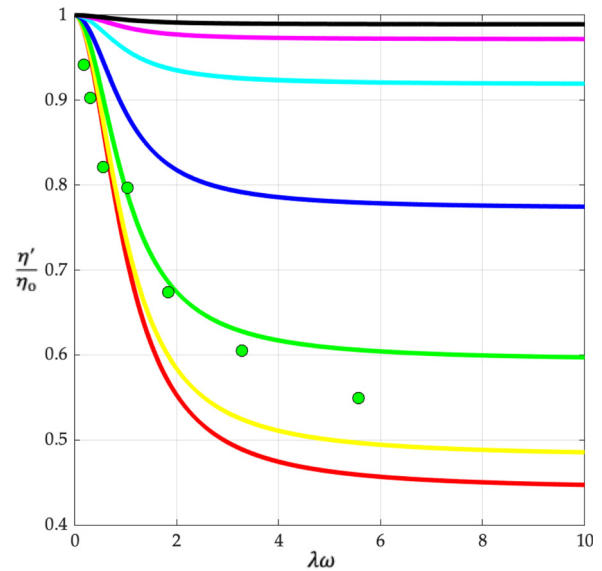


FIG. 21. $\eta'/\eta_0(\lambda\omega)$ from Eq. (164) for center-beaded and coreless tetrahedral star at varying θ_1 for prolate macromolecules [Eq. (156)] [black: $\theta_1 = \frac{1}{2}\Theta_i$; magenta: $\theta_1 = 0.90$ rad; cyan: $\theta_1 = 0.80$ rad; blue: $\theta_1 = \frac{1}{2}(\pi - \Theta_i)$ rad; green: $\theta_1 = 0.40$ rad; yellow: $\theta_1 = 0.20$ rad; red: $\theta_1 = 0.0$ rad] fitted to data for 4-arm star in Ref. 9 ($\eta_0 = 1.38 \times 10^5$ Pa s and $\lambda = 57.0$ s).

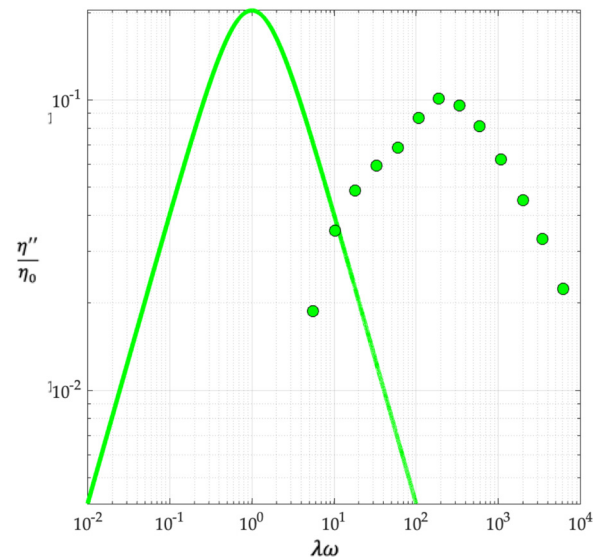


FIG. 22. $\eta''/\eta_0(\lambda\omega)$ from Eq. (165) for center-beaded and coreless tetrahedral stars at $\theta_1 = 0.40$ rad (prolate) for fitted values for 4-arm star of Fig. 21 ($\eta_0 = 1.38 \times 10^5$ Pa s and $\lambda = 57.0$ s).

18 April 2024 08:29:26

beaded or coreless tetrahedral star (Fig. 21). For these fitted values, Fig. 22 then tests Eq. (165). From Fig. 22, we learn that Eq. (165) overpredicts the peak η'' and underpredicts its frequency. From the fitted values of Fig. 21, for the center-beaded or coreless tetrahedral star, we get (see Table IV)

$$\frac{n^\ell \eta_0}{m \eta_0^\ell} = 15.31 \tag{182}$$

from fitting general rigid bead-rod theory for center-beaded or coreless tetrahedral star.

When you fit different structural formulas to the same η' data, you get different fitted values for η_0 , and thus different values for the scaled viscosity ratio $n^\ell \eta_0 / m \eta_0^\ell$. For instance, fitting reptation theory to the η' measurements of Ref. 9. Menezes gets $n^\ell \eta_0 / m \eta_0^\ell = 6.67$. By contrast, when we fit these same data from Eqs. (78) and (1), we get $n^\ell \eta_0 / m \eta_0^\ell = 14.09$ for center-beaded or center-ringed planar star.

A. Complex viscosity of a center-beaded planar star
($N_A = 4$)

Normalizing Eq. (77) with Eq. (1) gives Eq. (82), and when $N_A = 4$,

$$\frac{n^\ell \eta_0}{m \eta_0^\ell} = \frac{6(N_B + 1)}{4N_B + 1}, \tag{183}$$

whose lower asymptote ($N_B \rightarrow \infty$) is $3/2$ and whose upper bound ($N_B \rightarrow 0$) is 6 as shown in Fig. 23. This upper bound falls well below the measured value of 14.09 given in Eq. (181), from which we learn that branched polybutadiene of Refs. 8 and 9 does not behave as center-beaded planar star.

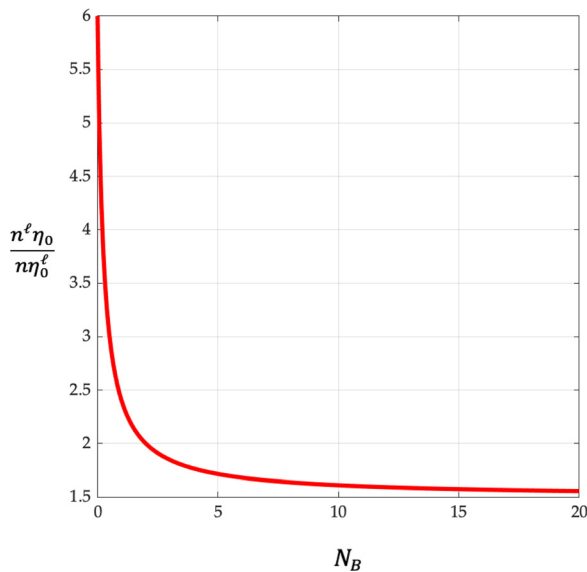


FIG. 23. $n^\ell \eta_0 / m \eta_0^\ell$ from Eq. (183) for center-beaded planar stars for 4-arm stars with varying branch length ($\eta_0 = 1.27 \times 10^5$ Pa s and $\lambda = 54.0$ s).

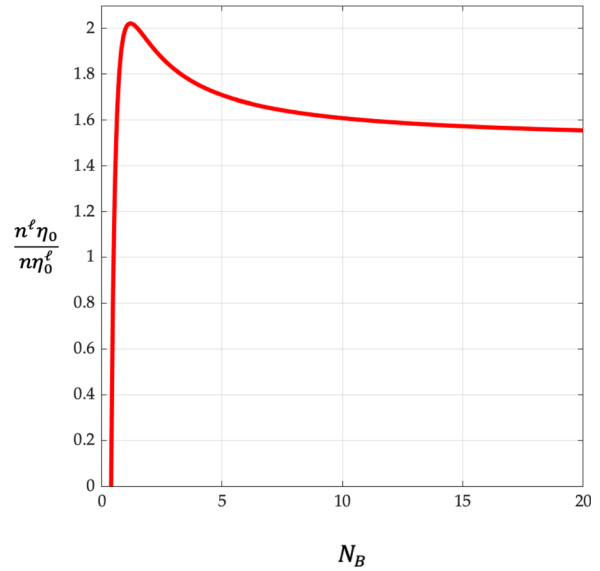


FIG. 24. $n^\ell \eta_0 / m \eta_0^\ell$ from Eq. (184) for center-ringed planar stars for 4-arm stars with varying branch length ($\eta_0 = 1.27 \times 10^5$ Pa s and $\lambda = 54.0$ s).

B. Complex viscosity of a center-ringed planar star
($N_A = 4$)

Equation (101) was normalized with Eq. (1), where $N_A = 4$, yielding

$$\frac{n^\ell \eta_0}{m \eta_0^\ell} = \frac{6(N_B + 1)}{4N_B + 1} - \frac{6}{N_B(4N_B + 1)(2N_B + 1)}, \tag{184}$$

whose upper bound ($N_B \rightarrow \infty$) is $3/2$ and whose lower bound ($N_B \rightarrow 0$) is $-\infty$, as shown in Fig. 24. This upper bound falls well below the measured value of 14.09 given in Eq. (181), from which we learn that branched polybutadiene of Refs. 8 and 9 does not behave as center-ringed planar star.

C. Complex viscosity of a center-beaded tetrahedral star
($N_A = 4$)

Equation (166) was normalized with Eq. (1), where $N_A = 4$, yielding

$$\frac{n^\ell \eta_0}{m \eta_0^\ell} = \frac{9(N_B + 1)}{(4N_B + 1)} \left\{ \frac{[\cos 2\theta_1 + 2](3 \cos 2\theta_1 + 1)^2 + (\cos 2\theta_1 + 3)[2 \cos 2\theta_1 - 5 \cos 4\theta_1 + 35]}{5(\cos 2\theta_1 + 3)^2} \right\}, \tag{185}$$

whose lower asymptote ($N_B \rightarrow \infty$) is

$$\frac{n^\ell \eta_0}{m \eta_0^\ell} = \frac{9}{4} \left\{ \frac{[\cos 2\theta_1 + 2](3 \cos 2\theta_1 + 1)^2 + (\cos 2\theta_1 + 3)[2 \cos 2\theta_1 - 5 \cos 4\theta_1 + 35]}{5(\cos 2\theta_1 + 3)^2} \right\}, \tag{186}$$

and whose upper bound ($N_B \rightarrow 0$) is

$$\frac{n^\ell \eta_0}{m \eta_0^\ell} = 9 \left\{ \frac{[\cos 2\theta_1 + 2](3 \cos 2\theta_1 + 1)^2 + (\cos 2\theta_1 + 3)[2 \cos 2\theta_1 - 5 \cos 4\theta_1 + 35]}{5(\cos 2\theta_1 + 3)^2} \right\}, \tag{187}$$

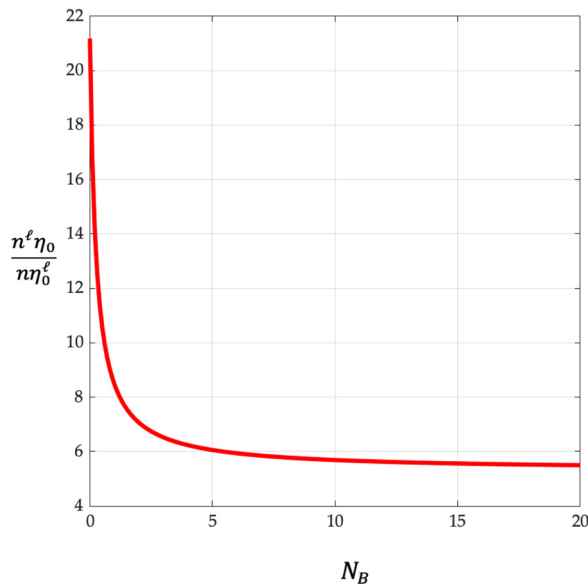


FIG. 25. $n^l \eta_0 / m \eta_0^l$ from Eq. (185) for center-beaded tetrahedral stars at $\theta_1 = 0.40$ for 4-arm stars with varying branch length ($\eta_0 = 1.38 \times 10^5$ Pa s, $\lambda = 57.0$ s).

as shown in Fig. 25. The measured value of 15.31 given in Eq. (182) falls within these bounds, from which we learn that branched polybutadiene of Refs. 8 and 9 behaves as an irregular center-beaded tetrahedral star at $\theta_1 = 0.40$ rad (23°), giving

$$N_B = 0.147 \tag{188}$$

from which we learn that, for 4-arm polybutadiene stars of molecular weight 200 000 g/gmol, this noninteger value obtains. Thus, $N_B = 1$ corresponds to 1 360 000 g/gmol, and so N_B will only be discrete for multiples of 1 360 000 g/gmol. Figure 26 illustrates the irregular tetrahedron with $\theta_1 = 0.40$ rad for a 4-arm polybutadiene star of molecular weight 4 080 000 g/gmol ($N_B = 3$). Since $\theta_1 = 0.40$ rad, we find that 4-arm polybutadiene star complex viscosity behavior is nearer the regular tetrahedron [$\theta_1 = \frac{1}{2}(\pi - \Theta_t)$] than the planar polygon ($\theta_1 = \frac{\pi}{2}$).

We thus find our general rigid bead-rod theory that most closely follows the measured complex viscosity behavior of the 4-arm star-branched polybutadiene solution is of the irregular center-beaded tetrahedral star at $\theta_1 = 0.40$ rad. We know that the specific 4-arm star-branched polybutadiene examined herein, has a silicon atom (and thus silicon tetrahedral bonding) at its core (Table I of Ref. 23). Silicon bonding is regular tetrahedral, thus with $\theta_1 = \frac{1}{2}(\pi - \Theta_t)$ rad = 0.62 rad,^{3,24,25} which is just above $\theta_1 = 0.40$ rad. In other words, in oscillatory shear flow, our 4-arm star-branched polybutadiene solution behavior is nearly tetrahedral, and specifically, just 0.22 rad (12°) on the prolate side of regular tetrahedral. So our 4 polybutadiene arms emanate nearly tetrahedrally from their silicon central core linking atom.

We next turn our attention to the Cole–Cole plots for which Fig. 1 of Ref. 26 applies where, for the center-beaded 4-arm star, b/ν is given by Eq. (150). Specifically, for $\theta_1 = 0.40$ rad and $N_B = 0.147$ [from Eq. (188)], we get $b/\nu = 0.0822$. Plotting the complex viscosity measurements of Fig. 3 of Ref. 8 (or Fig. 7.10 of Ref. 9) as a parametric plot in $\lambda\omega$ for $b/\nu = 0.0822$ yields Fig. 27. From Fig. 27, we learn that unlike for long-chain branching in molten polypropylene, general rigid

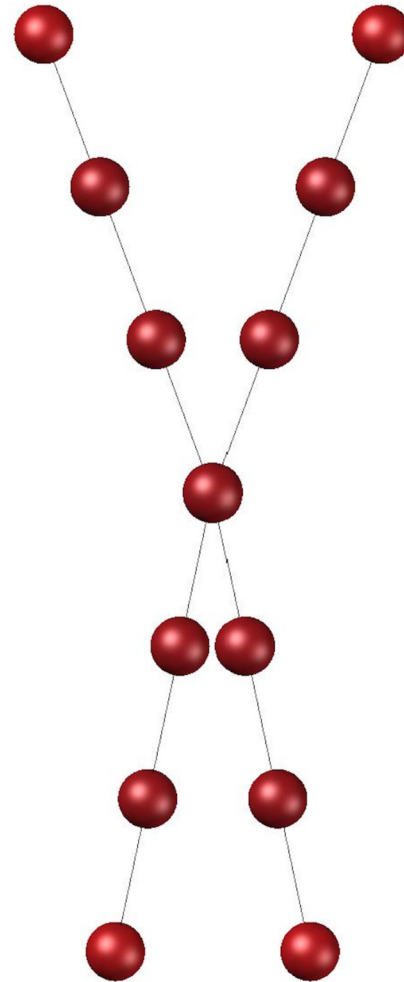


FIG. 26. Results for star-branched polybutadiene sample (ST1) explained with a 4-arm irregular center-beaded tetrahedral: $N_A = 4$, and $N_B = 3$ for $M_w = 4.08 \times 10^6$ g/gmol. R_i given by Eq. (143) with $\theta_1 = 0.40$ rad = 23° and $c = 1, \dots, N_B$.

bead-rod theory does not predict the Cole–Cole behavior of star-branched polybutadiene solution accurately (compare Fig. 27 with the good agreement in Fig. 18 of Ref. 26).

D. Complex viscosity of a coreless tetrahedral star ($N_A = 4$)

Equation (178) was normalized with Eq. (1), where $N_A = 4$, yielding

$$\frac{n^l \eta_0}{m \eta_0^l} = \frac{9[-1 + N_B(N_B + 1)(2N_B + 1)]}{N_B(4N_B + 1)(2N_B + 1)} \times \left\{ \frac{[\cos 2\theta_1 + 2](3 \cos 2\theta_1 + 1)^2}{+(\cos 2\theta_1 + 3)[2 \cos 2\theta_1 - 5 \cos 4\theta_1 + 35]}{5(\cos 2\theta_1 + 3)^2} \right\}, \tag{189}$$

whose upper bound ($N_B \rightarrow \infty$) is

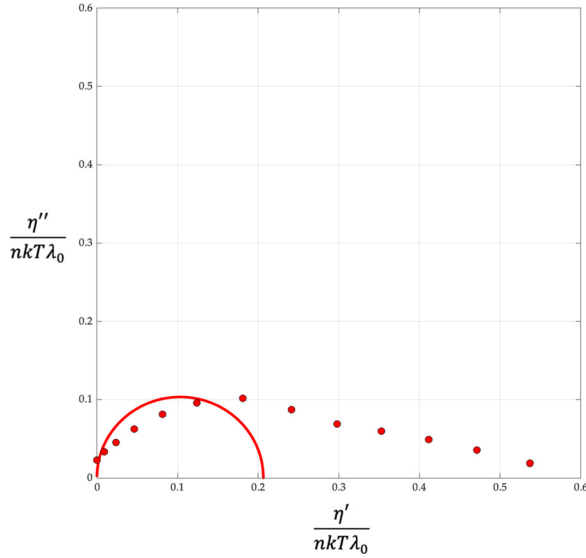


FIG. 27. Fit of dimensionless Cole–Cole plot of Eq. (62) of Ref. 26 for center-beaded polybutadiene for tetrahedral stars with $\theta_1 = 0.40$, $N_B = 0.147$, and $b/\nu = 0.0822$ ($\eta_0 = 1.38 \times 10^5$ Pa s, $\lambda = 57.0$ s).

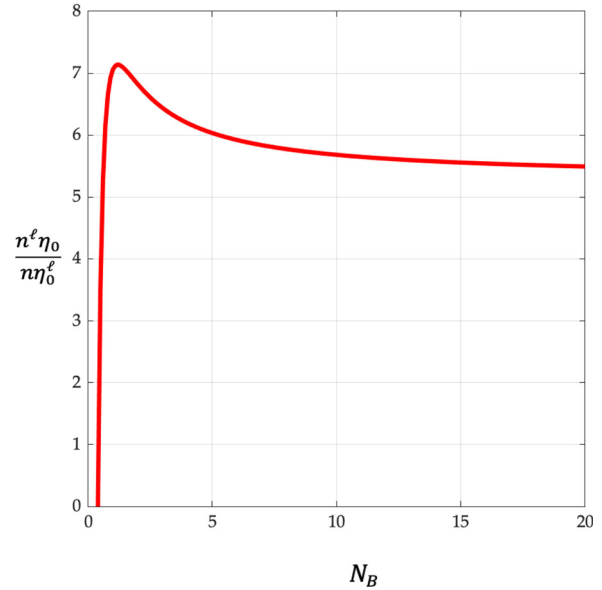


FIG. 28. $n^l \eta_0 / n \eta_0^l$ from Eq. (189) for coreless tetrahedral stars at $\theta_1 = 0.40$ for 4-arm stars with varying branch length ($\eta_0 = 1.38 \times 10^5$ Pa s, $\lambda = 57.0$ s).

$$\frac{n^l \eta_0}{n \eta_0^l} = \frac{9}{4} \left\{ \frac{[\cos 2\theta_1 + 2](3 \cos 2\theta_1 + 1)^2 + (\cos 2\theta_1 + 3)[2 \cos 2\theta_1 - 5 \cos 4\theta_1 + 35]}{5(\cos 2\theta_1 + 3)^2} \right\}, \quad (190)$$

and whose lower bound ($N_B \rightarrow 0$) is

$$\frac{n^l \eta_0}{n \eta_0^l} = -\infty, \quad (191)$$

TABLE V. Analytical results—planar $3 \leq N_A \leq 6$.

Center-beaded	Center-ringed
$I_1 \equiv \frac{N_A}{2} N_B(N_B + 1)(2N_B + 1)mL^2$	$I_1 \equiv mL^2[-1 + N_B(N_B + 1)(2N_B + 1)] \frac{N_A}{2}$
$I_2 \equiv \frac{N_A}{2} N_B(N_B + 1)(2N_B + 1)mL^2 = I_1$	$I_2 \equiv mL^2[-1 + N_B(N_B + 1)(2N_B + 1)] \frac{N_A}{2} = I_1$
$I_3 \equiv N_A N_B(N_B + 1)(2N_B + 1)mL^2$	$I_3 \equiv mL^2[-1 + N_B(N_B + 1)(2N_B + 1)]N_A$
$a \equiv \frac{7}{30} N_A N_B(N_B + 1)(2N_B + 1)$	$a \equiv \frac{7}{30} [-1 + N_B(N_B + 1)(2N_B + 1)]N_A$
$b \equiv \frac{3}{5}$	$b \equiv \frac{3}{5}$
$\nu \equiv \frac{12}{N_A N_B(N_B + 1)(2N_B + 1)}$	$\nu \equiv \frac{12}{[-1 + N_B(N_B + 1)(2N_B + 1)]N_A}$
$\frac{\lambda}{\lambda_0} \equiv N_A N_B(N_B + 1)(2N_B + 1)$	$\frac{\lambda}{\lambda_0} \equiv N_A[-1 + N_B(N_B + 1)(2N_B + 1)]$
$\frac{\eta_0}{nkT\lambda_0} = 2N_A N_B(N_B + 1)(2N_B + 1)$	$\frac{\eta_0}{nkT\lambda_0} = 2[-1 + N_B(N_B + 1)(2N_B + 1)]N_A$
$\frac{\eta'}{\eta_0} = \frac{7}{10} \left\{ 1 + \frac{3}{7} \left(\frac{1}{1 + (\lambda\omega)^2} \right) \right\}$	$\frac{\eta'}{\eta_0} = \frac{3}{10} \left\{ \frac{\lambda\omega}{1 + (\lambda\omega)^2} \right\}$
$\frac{n^l \eta_0}{n \eta_0^l} = \frac{12(N_B + 1)(2N_B + 1)}{(N_A N_B + 1)(N_A N_B + 2)}$	$\frac{n^l \eta_0}{n \eta_0^l} = \frac{12(N_B + 1)(2N_B + 1)}{(N_A N_B + 1)(N_A N_B + 2)} - \frac{12}{N_B(N_A N_B + 1)(N_A N_B + 2)}$
$\frac{\lambda}{\lambda^\ell} = \frac{6(N_B + 1)(2N_B + 1)}{(N_A N_B + 1)(N_A N_B + 2)}$	$\frac{\lambda}{\lambda^\ell} = \frac{6(N_B + 1)(2N_B + 1)}{(N_A N_B + 1)(N_A N_B + 2)} - \frac{6}{N_B(N_A N_B + 1)(N_A N_B + 2)}$

TABLE VI. Analytical results—planar $N_A \geq 7$.

Center-beaded	Center-ringed
$I_1 \equiv \frac{N_A}{8 \sin^2 \frac{\pi}{N_A}} N_B(N_B + 1)(2N_B + 1)mL^2$	$I_1 \equiv mL^2[-1 + N_B(N_B + 1)(2N_B + 1)] \frac{N_A}{8 \sin^2 \frac{\pi}{N_A}}$
$I_2 \equiv \frac{N_A}{8 \sin^2 \frac{\pi}{N_A}} N_B(N_B + 1)(2N_B + 1)mL^2 = I_1$	$I_2 \equiv mL^2[-1 + N_B(N_B + 1)(2N_B + 1)] \frac{N_A}{8 \sin^2 \frac{\pi}{N_A}} = I_1$
$I_3 \equiv \frac{N_A}{4 \sin^2 \frac{\pi}{N_A}} N_B(N_B + 1)(2N_B + 1)mL^2$	$I_3 \equiv mL^2[-1 + N_B(N_B + 1)(2N_B + 1)] \frac{N_A}{4 \sin^2 \frac{\pi}{N_A}}$
$a \equiv \frac{7}{120 \sin^2 \frac{\pi}{N_A}} N_A N_B(N_B + 1)(2N_B + 1)$	$a \equiv \frac{7}{120 \sin^2 \frac{\pi}{N_A}} [-1 + N_B(N_B + 1)(2N_B + 1)]N_A$
$b \equiv \frac{3}{5}$	$b \equiv \frac{3}{5}$
$\nu \equiv \frac{48 \sin^2 \frac{\pi}{N_A}}{N_A N_B(N_B + 1)(2N_B + 1)}$	$\nu \equiv \frac{48 \sin^2 \frac{\pi}{N_A}}{[-1 + N_B(N_B + 1)(2N_B + 1)]N_A}$
$\frac{\lambda}{\lambda_0} \equiv \frac{N_A N_B(N_B + 1)(2N_B + 1)}{4 \sin^2 \frac{\pi}{N_A}}$	$\frac{\lambda}{\lambda_0} \equiv \frac{[-1 + N_B(N_B + 1)(2N_B + 1)]N_A}{4 \sin^2 \frac{\pi}{N_A}}$
$\frac{\eta_0}{nkT\lambda_0} = \frac{1}{2 \sin^2 \frac{\pi}{N_A}} N_A N_B(N_B + 1)(2N_B + 1)$	$\frac{\eta_0}{nkT\lambda_0} = \frac{1}{2 \sin^2 \frac{\pi}{N_A}} [-1 + N_B(N_B + 1)(2N_B + 1)]N_A$
$\frac{\eta'}{\eta_0} = \frac{7}{10} \left\{ 1 + \frac{3}{7} \left(\frac{1}{1 + (\lambda\omega)^2} \right) \right\} \frac{\eta''}{\eta_0} = \frac{3}{10} \left\{ \frac{\lambda\omega}{1 + (\lambda\omega)^2} \right\}$	

as shown in Fig. 28. This upper bound falls well below the measured value of 15.31 given in Eq. (182), from which we learn that branched polybutadiene of Refs. 8 and 9 does not behave as coreless tetrahedral star.

VI. CONCLUSION

In this work, we proceed analytically from geometric expressions for the bead positions for whole classes of branched macromolecules [Eqs. (51), (54), (139), and (143)]. We arrive at the general expressions for the real and imaginary parts of the complex viscosity for planar stars of any number of branches or branch length for both center-

beaded [Eqs. (78) and (79)] and center-ringed [Eqs. (78) and (79)]. Tables V and VI summarize our results for planar stars. We find these planar predictions to disagree with the measured complex viscosity behavior of the polybutadiene solutions.

We thus next arrive at the general expressions for the real and imaginary parts of the complex viscosity for tetrahedral stars of any branch length or interior angle for both center-beaded [Eqs. (164) and (165)] and coreless [Eqs. (164) and (165)]. Table VII summarizes our results for tetrahedral stars. We find the measured complex viscosity behavior of polybutadiene solutions, one quadrafunctional star-branched, the other unbranched, of the same molecular weight

TABLE VII. Analytical results—tetrahedral.

Center-beaded	Coreless
$I_1 = 2mL^2 [1 + 2 \cos^2 \theta_1] N_B(N_B + 1)(2N_B + 1)$	$I_1 = 2mL^2 [1 + 2 \cos^2 \theta_1] [-1 + N_B(N_B + 1)(2N_B + 1)]$
$I_2 = 2mL^2 [1 + 2 \cos^2 \theta_1] N_B(N_B + 1)(2N_B + 1) = I_1$	$I_2 = 2mL^2 [1 + 2 \cos^2 \theta_1] [-1 + N_B(N_B + 1)(2N_B + 1)] = I_1$
$I_3 = 4mL^2 \sin^2 \theta_1 N_B(N_B + 1)(2N_B + 1)$	$I_3 = 4mL^2 \sin^2(\theta_1) [-1 + N_B(N_B + 1)(2N_B + 1)]$
$a \equiv \frac{N_B(N_B + 1)(2N_B + 1)}{15(\cos 2\theta_1 + 3)} [2 \cos 2\theta_1 - 5 \cos 4\theta_1 + 35]$	$a \equiv \frac{[-1 + N_B(N_B + 1)(2N_B + 1)]}{15(\cos 2\theta_1 + 3)} [2 \cos 2\theta_1 - 5 \cos 4\theta_1 + 35]$
$b \equiv \frac{3(3 \cos^2 \theta_1 - 1)^2}{5(\cos^2 \theta_1 + 1)^2} = \frac{3(3 \cos 2\theta_1 + 1)^2}{5(\cos 2\theta_1 + 3)^2}$	

TABLE VII. (Continued.)

Center-beaded	Coreless
$\nu \equiv \frac{3}{[\cos 2\theta_1 + 2]N_B(N_B + 1)(2N_B + 1)}$	$\nu \equiv \frac{3}{[\cos 2\theta_1 + 2][-1 + N_B(N_B + 1)(2N_B + 1)]}$
$\frac{\lambda}{\lambda_0} \equiv 4[\cos(2\theta_1) + 2]N_B(N_B + 1)(2N_B + 1)$	$\frac{\lambda}{\lambda_0} \equiv 4[\cos(2\theta_1) + 2][-1 + N_B(N_B + 1)(2N_B + 1)]$
$\frac{\eta_0}{nkT\lambda_0} = 6 \frac{N_B(N_B + 1)(2N_B + 1)}{15(\cos(2\theta_1) + 3)} [2 \cos(2\theta_1) - 5 \cos(4\theta_1) + 35]$ $\times \left\{ 1 + \frac{6[\cos(2\theta_1) + 2](3 \cos(2\theta_1) + 1)^2}{(\cos(2\theta_1) + 3)[2 \cos(2\theta_1) - 5 \cos(4\theta_1) + 35]} \right\}$	$\frac{\eta_0}{nkT\lambda_0} = 6 \frac{[-1 + N_B(N_B + 1)(2N_B + 1)]}{15(\cos(2\theta_1) + 3)} [2 \cos(2\theta_1) - 5 \cos(4\theta_1) + 35]$ $\times \left\{ 1 + \frac{6[\cos(2\theta_1) + 2](3 \cos(2\theta_1) + 1)^2}{(\cos(2\theta_1) + 3)[2 \cos(2\theta_1) - 5 \cos(4\theta_1) + 35]} \right\}$
$\frac{\eta'}{\eta_0} = \frac{1 + \frac{6[\cos(2\theta_1) + 2](3 \cos(2\theta_1) + 1)^2}{(\cos(2\theta_1) + 3)[2 \cos(2\theta_1) - 5 \cos(4\theta_1) + 35]} \left(\frac{1}{1 + (\lambda\omega)^2} \right)}{1 + \frac{6[\cos(2\theta_1) + 2](3 \cos(2\theta_1) + 1)^2}{(\cos(2\theta_1) + 3)[2 \cos(2\theta_1) - 5 \cos(4\theta_1) + 35]}}$	$\frac{\eta'}{\eta_0} = \frac{1 + \frac{6[\cos(2\theta_1) + 2](3 \cos(2\theta_1) + 1)^2}{(\cos(2\theta_1) + 3)[2 \cos(2\theta_1) - 5 \cos(4\theta_1) + 35]} \left(\frac{1}{1 + (\lambda\omega)^2} \right)}{1 + \frac{6[\cos(2\theta_1) + 2](3 \cos(2\theta_1) + 1)^2}{(\cos(2\theta_1) + 3)[2 \cos(2\theta_1) - 5 \cos(4\theta_1) + 35]}}$
$\frac{\eta''}{\eta_0} = \frac{\frac{6[\cos 2\theta_1 + 2](3 \cos 2\theta_1 + 1)^2}{(\cos 2\theta_1 + 3)[2 \cos 2\theta_1 - 5 \cos 4\theta_1 + 35]} \frac{\lambda\omega}{1 + (\lambda\omega)^2}}{1 + \frac{6[\cos 2\theta_1 + 2](3 \cos 2\theta_1 + 1)^2}{(\cos 2\theta_1 + 3)[2 \cos 2\theta_1 - 5 \cos 4\theta_1 + 35]}}$	$\frac{\eta''}{\eta_0} = \frac{\frac{6[\cos 2\theta_1 + 2](3 \cos 2\theta_1 + 1)^2}{(\cos 2\theta_1 + 3)[2 \cos 2\theta_1 - 5 \cos 4\theta_1 + 35]} \frac{\lambda\omega}{1 + (\lambda\omega)^2}}{1 + \frac{6[\cos 2\theta_1 + 2](3 \cos 2\theta_1 + 1)^2}{(\cos 2\theta_1 + 3)[2 \cos 2\theta_1 - 5 \cos 4\theta_1 + 35]}}$
$\frac{n^\ell \eta_0}{m \eta_0^\ell} = \frac{72N_B(N_B + 1)(2N_B + 1)}{N_A N_B(N_A N_B + 1)(N_A N_B + 2)}$ $\times \left\{ \frac{[\cos 2\theta_1 + 2](3 \cos 2\theta_1 + 1)^2 + (\cos 2\theta_1 + 3) \left[\frac{2 \cos 2\theta_1}{-5 \cos 4\theta_1 + 35} \right]}{5(\cos 2\theta_1 + 3)^2} \right\}$	$\frac{n^\ell \eta_0}{m \eta_0^\ell} = \frac{72[-1 + N_B(N_B + 1)(2N_B + 1)]}{N_A N_B(N_A N_B + 1)(N_A N_B + 2)}$ $\times \left\{ \frac{[\cos 2\theta_1 + 2](3 \cos 2\theta_1 + 1)^2 + (\cos 2\theta_1 + 3) \left[\frac{2 \cos 2\theta_1 - 5 \cos 4\theta_1 + 35}{5(\cos 2\theta_1 + 3)^2} \right]}{5(\cos 2\theta_1 + 3)^2} \right\}$
$\frac{\lambda}{\lambda^\ell} = \frac{24[\cos(2\theta_1) + 2]N_B(N_B + 1)(2N_B + 1)}{N_A N_B(N_A N_B + 1)(N_A N_B + 2)}$	$\frac{\lambda}{\lambda^\ell} = \frac{24[\cos(2\theta_1) + 2][-1 + N_B(N_B + 1)(2N_B + 1)]}{N_A N_B(N_A N_B + 1)(N_A N_B + 2)}$

($M_w = 200\,000$ g/gmol) to agree with the predictions of general rigid bead-rod theory (Fig. 21). Specifically, we learn that when general rigid bead-rod theory is applied to our quadrafunctional polybutadiene, a slightly irregular center-beaded tetrahedron of interior angle 134° is required (with $1\,360\,000$ g/gmol per bead) to describe accurately the

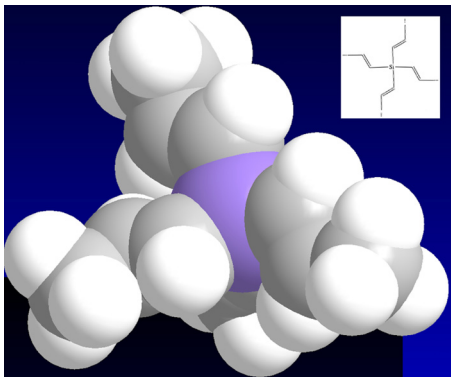


FIG. 29. Space filling representation with skeletal structural formula³¹ inset of silicon-linked 4-arm tetrahedral *cis*-polybutadiene star ($N_A = 4$) with its first 4 *cis*-isomers ($M_w = 192.38$ g/gmol) produced by lithium catalyzed anionic polymerization followed by silicon chloride linking.^{3,8,9,24}

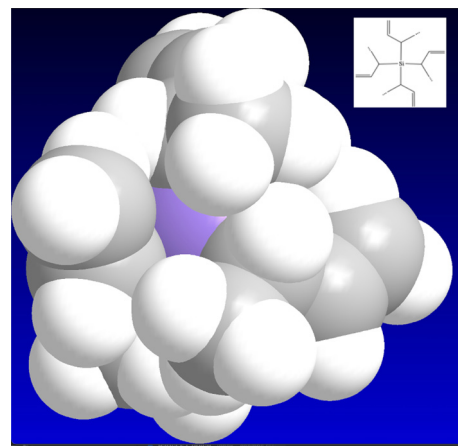


FIG. 30. Space filling representation with skeletal structural formula³¹ inset of silicon tetrachloride-linked 4-arm tetrahedral *trans*-polybutadiene star ($N_A = 4$) with its first 4 *trans*-isomers ($M_w = 248.49$ g/gmol) produced by lithium catalyzed anionic polymerization followed by silicon chloride linking.^{3,8,9,24}

TABLE VIII. Worked example ($N_A = 4$).

Macromolecule structure	Concentration factor
Center-beaded planar star	$\frac{n^\ell \eta_0}{n \eta_0^\ell} = \frac{6(N_B + 1)}{4N_B + 1}$
Center-ringed planar star	$\frac{n^\ell \eta_0}{n \eta_0^\ell} = \frac{6(N_B + 1)}{4N_B + 1} - \frac{6}{N_B(4N_B + 1)(2N_B + 1)}$
Center-beaded tetrahedral star	$\frac{n^\ell \eta_0}{n \eta_0^\ell} = \frac{9(N_B + 1)}{(4N_B + 1)} \left\{ \frac{[\cos 2\theta_1 + 2](3 \cos 2\theta_1 + 1)^2 + (\cos 2\theta_1 + 3)[2 \cos 2\theta_1 - 5 \cos 4\theta_1 + 35]}{5(\cos 2\theta_1 + 3)^2} \right\}$
Coreless tetrahedral star	$\frac{n^\ell \eta_0}{n \eta_0^\ell} = \frac{9[-1 + N_B(N_B + 1)(2N_B + 1)]}{N_B(4N_B + 1)(2N_B + 1)} \left\{ \frac{[\cos 2\theta_1 + 2](3 \cos 2\theta_1 + 1)^2 + (\cos 2\theta_1 + 3)[2 \cos 2\theta_1 - 5 \cos 4\theta_1 + 35]}{5(\cos 2\theta_1 + 3)^2} \right\}$

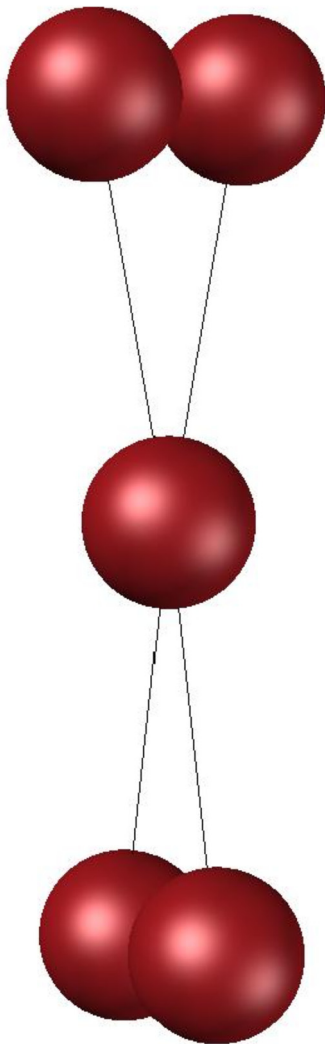


FIG. 31. Five-bead quarter-twisted osculated dumbbell.

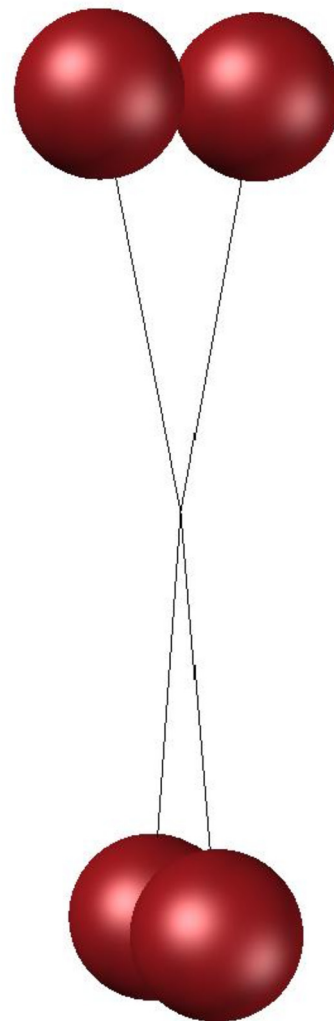


FIG. 32. Four-bead quarter-twisted osculated dumbbell.

real part of its complex viscosity behavior (see Fig. 26). Interestingly, this is consistent with its silicon-centered (and thus tetrahedral) chemistry (see Figs. 29 and 30). However, this same general rigid bead-rod theory overpredicts the peak of the imaginary part of its complex viscosity and underpredicts the peak frequency (see Fig. 22). We attribute this discrepancy to branch length dispersity, be it from branch-to-branch on the same star or between stars. To handle such mixtures of different species we can rewrite Eqs. (164) and (165) for a dispersed system of S species (see problem 14 C.2 of Ref. 7, see also Sec. 26 of Ref. 19). We leave this for another day (Table VIII).

For this paper, Refs. 8 and 9 provided a unique comparison of the complex viscosities of polymer solutions, star-branched vs unbranched, of the same molecular weight. We know of no other measurements of star-branched vs unbranched, of the same molecular weight of any polymer.^{21,22,27,28}

Our work on tetrahedral stars uncovers a new pair of dumbbells: the five-bead or four-bead quarter-twisted osculated dumbbells shown, respectively, in Figs. 31 and 32. For these, we subject Eqs. (164) and (165) to the osculation constraint $\sin \theta_1 = d/2L$, producing new dumbbells with exactly two parameters: d and L . We have thus uncovered two new counterparts to the rigid dumbbell. We leave their exploration for future work.

From Fig. 11, we learned that the lopsidedness of tetrahedral macromolecules, $2b/av$, vs θ_1 is curiously asymmetric. With some effort, employing Eqs. (152) and (148), we can transform the function illustrated in Fig. 11 to a Fourier series. We leave this task for another day.

We observe that recent work on ancient polymers transported by meteorites may also be 4-arm stars of structures more complex than our tetrahedral polybutadienes (Fig. 9 of Ref. 29). Called *stacked tetraskelelia*, we leave the evaluation of their complex viscosity in solution, from first principles and by the method of general rigid bead-rod theory for another day.

When using the references cited herein, it is best to be mindful of corresponding ganged errata in Ref. 30.

ACKNOWLEDGMENTS

Giacomin is indebted to the Faculty of Applied Science and Engineering of Queen's University at Kingston, for its support through a Research Initiation Grant (RIG). This research was undertaken, in part, thanks to support from the Canada Research Chairs program of the Government of Canada for the Natural Sciences and Engineering Research Council of Canada (NSERC) Tier 1 Canada Research Chair in Rheology. This research was also undertaken, in part, thanks to support from the Society of Plastics Engineers in the form of the Lew Erwin Extrusion Division Scholarship awarded to Coombs.

We thank Professor Wesley Roth Burghardt of Northwestern University for locating and providing the Menezes Thesis.⁹

DATA AVAILABILITY

The data that support the findings of this study are available within the article.

REFERENCES

- M. A. Kansa, A. J. Giacomin, C. Saengow, and J. H. Piette, "Macromolecular architecture and complex viscosity," *Phys. Fluids* **31**(8), 087107 (2019); Errata: Eq. (21) should be " $a^2v^2 + \frac{2}{3}(6b-9)av + \frac{1}{5}(36b^2 - 123 + 81) = 0$ "; in Table XIV, $n_0 - n_s$ should be $\eta_0 - \eta_s$; in Table XV, $\psi_{1,0}$ should be $\Psi_{1,0}$, and nKT should be

nKT ; in Table IV, Macromolecule 21 entry should be $[-\frac{1}{2}L, -\frac{\sqrt{3}}{2}L, 0]$; $[L, 0, 0]$; $[-\frac{1}{2}L, \frac{\sqrt{3}}{2}L, 0]$ and macromolecule 17 entry should be multiplied by L ; in Eq. (44), η'' should be $2\eta''$.

- M. A. Kansa, "Polymeric liquid behavior in oscillatory shear flow," M.A.Sc. thesis (Queen's University, Kingston, Ontario, 2019).

- W. E. Rochefort, G. G. Smith, H. Rachapudy, V. R. Raju, and W. W. Graessley, "Properties of amorphous and crystallizable hydrocarbon polymers. II. Rheology of linear and star-branched polybutadiene," *J. Polym. Sci.* **17**(1), 1197–1210 (1979).

- M. A. Kansa, A. J. Giacomin, and C. Saengow, "Large-amplitude oscillatory shear flow loops for long-chain branching from general rigid bead-rod theory," *Phys. Fluids* **32**(5), 053102 (2020).

- M. A. Kansa and A. J. Giacomin, "Polymer branching and first normal stress differences in small-amplitude oscillatory shear flow," *Can. J. Chem. Eng.* **98**(7), 1444–1455 (2020); Erratum: In Eq. (24), " Ψ'' " should be " Ψ' ".

- K. El Haddad, C. Aumnate, C. Saengow, M. A. Kansa, S. J. Coombs, and A. J. Giacomin, "Complex viscosity of graphene suspensions," PRG Report No. QU-CHEE-PRGTR-2021-80 (Queen's University, Kingston, Canada, 2021).

- R. B. Bird, C. F. Curtiss, R. C. Armstrong, and O. Hassager, *Dynamics of Polymeric Liquids*, 2nd ed. (Wiley, New York, 1987), Vol. 2.

- E. V. Menezes and W. W. Graessley, "Nonlinear rheological behavior of polymer systems for several shear-flow histories," *J. Polym. Sci.* **20**, 1817–1833 (1982).

- E. V. Menezes, "Rheological properties of polymers in the linear and nonlinear viscoelastic regimes," Ph.D. thesis (Northwestern University, Evanston, Illinois, 1980).

- R. B. Bird, O. Hassager, R. C. Armstrong, and C. F. Curtiss, *Dynamics of Polymeric Liquids*, 1st ed. (John Wiley and Sons, Inc., New York, 1977).

- J. H. Piette, L. M. Jbara, C. Saengow, and A. J. Giacomin, "Exact coefficients for rigid dumbbell suspensions for steady shear flow material function expansions," *Phys. Fluids* **31**(2), 021212 (2019); Erratum: Above Eq. (83), "one other" should be "one other use."

- L. G. Leal and E. J. Hinch, "The rheology of a suspension of nearly spherical particles subject to Brownian rotations," *J. Fluid Mech.* **55**(4), 745–765 (1972).

- M. A. Kansa and A. J. Giacomin, "Van Gurp-Palmen relations for long-chain branching from general rigid bead-rod theory," *Phys. Fluids* **32**(3), 033101 (2020).

- R. B. Bird, A. J. Giacomin, A. M. Schmalzer, and C. Aumnate, "Dilute rigid dumbbell suspensions in large-amplitude oscillatory shear flow: shear stress response," *J. Chem. Phys.* **140**(7), 074904 (2014); Erratum: Ganged after Ref. 116 of Ref. 32 below.

- O. Hassager, "Kinetic theory and rheology of bead-rod models for macromolecular solutions. II. Linear unsteady flow properties," *J. Chem. Phys.* **60**(10), 4001–4008 (1974); Errata: In Eq. (2) " $1/2$ " should be " $-1/2$ " and " \ll " should be " \gg ".

- A. Gemant, "Komplexe Viskosität," *Naturwissenschaften* **23**(25), 406–407 (1935).

- A. Gemant, "The conception of a complex viscosity and its application to dielectrics," *Trans. Faraday Soc.* **31**(175), 1582–1590 (1935).

- R. B. Bird and A. J. Giacomin, "Who conceived the complex viscosity?," *Rheol. Acta* **51**(6), 481–486 (2012).

- R. B. Bird, H. R. Warner, Jr., and D. C. Evans, "Kinetic theory and rheology of dumbbell suspensions with Brownian motion," *Fortschr. Hochpoly.-Forsch. (Adv. Polym. Sci.)* **8**, 1–90 (1971).

- R. B. Bird, W. E. Stewart, and E. N. Lightfoot, *Transport Phenomena*, 2nd ed. (John Wiley and Sons, Inc., New York, 2007).

- A. Y. Malkin, M. Y. Polyakova, A. V. Andrianov, I. V. Meshkov, and A. M. Muzafarov, "Viscosity and viscoelasticity of liquid nanoparticles with polymeric matrix," *Phys. Fluids* **31**(8), 083104 (2019).

- K. Hyun, E. S. Baik, K. H. Ahn, S. J. Lee, M. Sugimoto, and K. Koyama, "Fourier-transform rheology under medium amplitude oscillatory shear for linear and branched polymer melts," *J. Rheol.* **51**(6), 1319 (2007).

- V. R. Raju, E. V. Menezes, G. Marin, and W. W. Graessley, "Concentration and molecular weight dependence of viscoelastic properties in linear and star polymers," *Macromolecules* **14**(6), 1668–1676 (1981).

- N. Hadjichristidis, S. Pispas, H. Iatrou, and M. Pitsikalis, "Linking chemistry and anionic polymerization," *Curr. Org. Chem.* **6**(2), 155–176 (2002).

- ²⁵Y. Wang, Y. Xie, P. Wei, H. F. Schaefer III, and G. H. Robinson, “Abnormal carbene—silicon halide complexes,” *Dalton Trans.* **45**(11), 5941–5944 (2016).
- ²⁶S. J. Coombs, M. A. Kanso, and A. J. Giacomin, “Cole–Cole relation for long-chain branching from general rigid bead-rod theory,” *Phys. Fluids* **32**(9), 093106 (2020).
- ²⁷P. Bačová, E. Gkolfi, L. G. D. Hawke, and V. Harmandraris, “Dynamical heterogeneities in non-entangled polystyrene and poly(ethylene oxide) star melts,” *Phys. Fluids* **32**(12), 127117 (2020).
- ²⁸K. Yasuda, R. C. Armstrong, and R. E. Cohen, “Shear flow properties of concentrated solutions of linear and star branched polystyrenes,” *Rheol. Acta* **20**, 163–178 (1981).
- ²⁹J. E. M. McGeoch and M. W. McGeoch, “Structural organization of space polymers,” *Phys. Fluids* **33**(6), 067118 (2021).
- ³⁰S. J. Coombs, M. A. Kanso, K. El Haddad, and A. J. Giacomin, “Complex viscosity of star-branched macromolecules from analytical general rigid bead-rod theory,” PRG Report No. 079, QU-CHEE-PRGTR–2021–79 (Polymers Research Group, Chemical Engineering Dept., Queen’s University, Kingston, Canada, 2021), pp. 0–76.
- ³¹PerkinElmer Informatics, *PerkinElmer Chem3D Pro (Version 20.1.1.125)* (PerkinElmer Informatics, Columbus, 1985).
- ³²C. Saengow, A. J. Giacomin, and C. Kositawong, “Exact analytical solution for large-amplitude oscillatory shear flow from Oldroyd 8-constant framework: Shear stress,” *Phys. Fluids* **29**(4), 043101 (2017); Erratum: In column 4 of rows 12 and 13 of Table IV $\lambda_2 = \mu_0 = \mu_1$ should be $\mu_1 = -\lambda_1$; $\lambda_2 = \mu_0$ and $\mu_1 = \lambda_1$; $\lambda_2 = \mu_0$.